DETERMINATION OF THE EFFECTS OF CARBON BLACK AND CROSSLINKING AGENT ON CURING OF EPOXY

LYE YON KAI

A project report submitted in partial fulfilment of the requirements for the award of Bachelor of Engineering (Hons.) Chemical Engineering

Faculty of Engineering and Science
Universiti Tunku Abdul Rahman

SEPTEMBER 2012

DECLARATION

I hereby declare that this project report is based on my original work except for citations and quotations which have been duly acknowledged. I also declare that it has not been previously and concurrently submitted for any other degree or award at UTAR or other institutions.

Signature : _____

Name : LYE YON KAI

ID No. : 09 UEB 00022

Date : 27 AUGUST 2012

APPROVAL FOR SUBMISSION

I certify that this project report entitled **"DETERMINATION OF THE EFFECTS OF CARBON BLACK AND CROSSLINKING AGENT ON CURING OF EPOXY"** was prepared by **LYE YON KAI** has met the required standard for submission in partial fulfilment of the requirements for the award of Bachelor of Engineering (Hons.) Chemical Engineering at Universiti Tunku Abdul Rahman.

Approved by,

Signature : _____

Supervisor : Ir. Dr. Tee Tiam Teng

Date : _____

Specially dedicated to my beloved Lecturers, father, mother and friends

ACKNOWLEDGEMENTS

I would like to thank everyone who had contributed to the successful completion of this project. I would like to express my gratitude to my research supervisor, Ir. Dr. Tee Tiam Ting for his invaluable advice, guidance and his enormous patience throughout the development of the research.

Besides that, I would like to express gratitude to Dr Lee Tin Sin and Ms Bee Soon Tueen who gave me a lot of idea and show me direction to conduct my research on this title. Deepest thank you send to lab assistance who guided me on experimental instruments.

In addition, I would also like to express my gratitude to my loving parent and friends who had helped and given me encouragement.

DETERMINATION OF THE EFFECTS OF CARBON BLACK AND CROSSLINKING AGENT ON CURING OF EPOXY

ABSTRACT

Two types of Carbon Black (CB N550 and N774) were added into epoxy resin at different weight percentages with a curing agent to study the effect on morphology and rheological properties. The distribution and dispersion of CB in epoxy was observed by using scanning electron microscopy (SEM). Microstructure and crystallinity were investigated by X-ray diffractometer (XRD). Viscosity and viscoelastic behaviour such as storage modulus (G'), loss modulus (G") and phase angle were measured by a rheometer. The result indicates that the crystallinity of 5 wt.% N550-epoxy composites is 5.12 % compare to 7.21 % of neat epoxy. Besides effect of concentration, smaller particles size of CB (N550) decrease the crystallinity of epoxy more significantly because it tend to disperse better in epoxy system. In addition, with present of cross linking agent and increasing of CB weight percentage, epoxy shows higher viscosity, G' and G" values. Hence, 5 wt.% of CB-epoxy composites gave the highest value of viscosity, G' and G" at initial and after 1 hour of curing. Although smaller filler sizes increase the rheological values outstandingly at initial reading compare to large particles but it slow down the curing process more significantly due to its small particle size, large surface area and high dispersion rate. On the other hand, cross linking agent present in the composites greatly increase the rheological properties after 1 hour of curing time. In conclusion, crystallinity of epoxy decreases with additional of CB particles but viscosity, G' and G" of epoxy are increase by adding CB. However, epoxy with larger particle size filler shows higher values of viscosity, G' and G" after 1 hour curing time compare to small particle filler.

TABLE OF CONTENTS

LIST OF TABLES

LIST OF FIGURES

LIST OF SYMBOLS / ABBREVIATIONS

γ	shear strain, %
2θ	diffractional peak, °
G'	storage modulus, Pa.s
G"	loss modulus, Pa.s
Wt.%	weight percent, %

AEAPTS	N-(2-aminoethyl)-3- aminopropyltrimethoxysilane
ASTM	American Society for Testing and Materials
BET	Brunauer, Emmett and Teller
CB	carbon black
CTE	coefficient of thermal expansion
DGEBA	diglycidyl ether of bisphenol-A
DTG	derivative thermogravimetric analysis
EDX	energy-dispersive X-ray spectroscopy
ENP	elastomeric nanoparticles
FTIR	fourier transform infrared spectrometer
HAF	high-abrasion furnace black
ICA	isotropic conductive adhesives
IPN	interpenetrating polymer networks
ISAF	intermediate superabrasion furnace black
MMT	montmorillonite
MRE	magnetorheological elastomers
RMS	root-mean-square
SAF	superabrasion furnace black
SEM	scanning electron microscopy
St-BA-EGDMA	styrene-butylacrylate-ethylenglycolimethacrylate
TGA	thermogravimetric analysis

XRD	X-ray diffraction

LIST OF APPENDICES

CHAPTER 1

INTRODUCTION

1.1 Background

Epoxy which also known as polyepoxide is one of the most important thermosetting polymer formed from reaction of an epoxide resin with polyamine hardener (cross linking agent). Epoxies are mainly used in coating, printed circuits, high performance adhesives, construction, insulation, reinforcing and a lot others engineering fields due to the good properties such as excellent moisture, solvent and chemical resistance, low shrinkage after cure, superior electrical and mechanical properties, good adhesion to many substrates.

However in most of the application, epoxy shares some common weaknesses which are low impact strength and brittle with poor resistance to crack propagation. To increase lifetime of coating, epoxy resin should improve combined physical, mechanical, thermal properties which are good thermal stability, low water absorption, low coefficient of thermal expansion (CTE) and low internal stress, high mechanical strength and low modulus. Several way are recommended to achieve the target which include (1)chemical modification of the epoxy, (2)increasing the molecular weight of epoxy, (3)lowering the cross-link density of matrix, (4)incorporation of a dispersed toughener phase in the cured polymer matrix, and (5)incorporation of inorganic materials into the neat resin (Khoee & Hassani, 2010)

Polymers composites with inorganic materials grab attention and interest of researcher recently because it is not only enhancing the properties of epoxy yet might generate certain new properties.

Carbon black (CB) is a kind of black powdered inorganic particles produced by incomplete combustion or thermal cracking of hydrocarbons under strictly controlled conditions, main components of which are C and a little O, H and S elements. The shape of particle is almost spherical and grain size of which is in the range of 0.1 to 500 nm. It is often used as anti-static and conducting materials, self-controlling temperature exothermic material, protective coatings, pressure-sensitive conduction resin, gas sensitive electric resistance and electromagnetic wave screening. It greatly increases resistance to wear and abrasion when add into polymer as a reinforcing filler.

By only adding a small amount of CB content, clear improvement in thermal and mechanical properties of epoxy can be observed. But the enhancement will be limiting by carbon black itself after exceed a certain amount. The highest adhesion strength was obtained with 20 wt% of elastomeric nanoparticles (Khoee & Hassani, 2010).

1.2 Problem Statements

There were problem statements found in this research when determining the effect of CB and cross linking agent:

1) What is the effect of cross linking agent onto the viscosity and viscoelastic behaviour of Epoxy?
2) What is the effect of cross linking agent onto the structure and bonding of epoxy?
3) What is the effect of vary amount and types of carbon black (CB) onto the viscosity and viscoelastic behaviour of Epoxy?

4) What is the effect of carbon black onto the structure and bonding of epoxy derived from various type and dose of carbon black (CB)?

1.3 Objective

In order to determine the effect of CB and cross linking agent onto the morphological and rheological properties of epoxy, following objectives had been targeted:

1) To compare the rheological properties (viscosity and viscoelastic behaviour) of epoxy before and after adding carbon black (CB).
2) To determine the changing of rheological properties (viscosity and viscoelastic behaviour) of epoxy with cross linking agent.
3) To compare the structure of epoxy before and after adding carbon black (CB).
4) To determine the effect of cross linking agent on structure and bonding of epoxy.

1.4 Scope

Several scopes of studies were targeted in order to achieve the target of this research which stated as below:

1) Study the effect of carbon black (CB) toward rheological properties (viscosity and viscoelastic behaviour) of epoxy base on different type and various amount of carbon black (CB) compound.
2) Study the effect of cross linking agent on rheological properties (viscosity and viscoelastic behaviour) of epoxy.
3) Study the changing of structure and bonding of epoxy after adding carbon black (CB).
4) Study the structure and bonding change of epoxy with existing of cross linking agent.

CHAPTER 2

LITERATURE REVIEW

2.1 Epoxy

Epoxy resins are the most common polymer matrix used for coating and liquid adhesives. The epoxies complex form as diglycidyl ether of bisphenol-A (DGEBA), which are synthesized by reacting bisphenol A and epichlorohydrin. DGEBA epoxy has an epoxide functionality of 2 for its average molecular weight of 380. The main components of an epoxy system are resin and the filler. Sometimes an accelerator is added to facilitate curing, results to the desired reaction products at desired temperatures. Notice the bisphenol A resin contains active three-member rings. Ring opening reactions with hardeners produce highly cross-linked structures in a curing process. Several types of cross linking agent have been found effective which lead to different rates of curing, reaction products and properties. The cross linking agent can be grouped into three major categories: catalytic (Lewis acids and bases), amines (aliphatic and aromatic), and anhydrides (Durairaj, Lam, Ekere, & Malik, 2010). These are irreversible chemical processes that cannot be repeated. Epoxy as one of the thermoset materials will not flow once cross-linked and they are normally rigid. Thermoset can be divided into a variety of resins such as unsaturated polyester, phenol formaldehyde and epoxy. Furthermore, thermoset contains a wide range of chemical reactions and conversion processes, thereof very useful in plastics industry and occupy 15 % of it (Harper, 2006). Figure 2.1 shows the schematic representation of the curing reaction of epoxy resins (*R–NH_2=$H_2NCH_2CH_2NH_2$, $H_2NCH_2CH_2HNCH_2CH_2NH_2$, $H_2N(CH_2CH_2HN)_2CH_2CH_2Nh_2$).

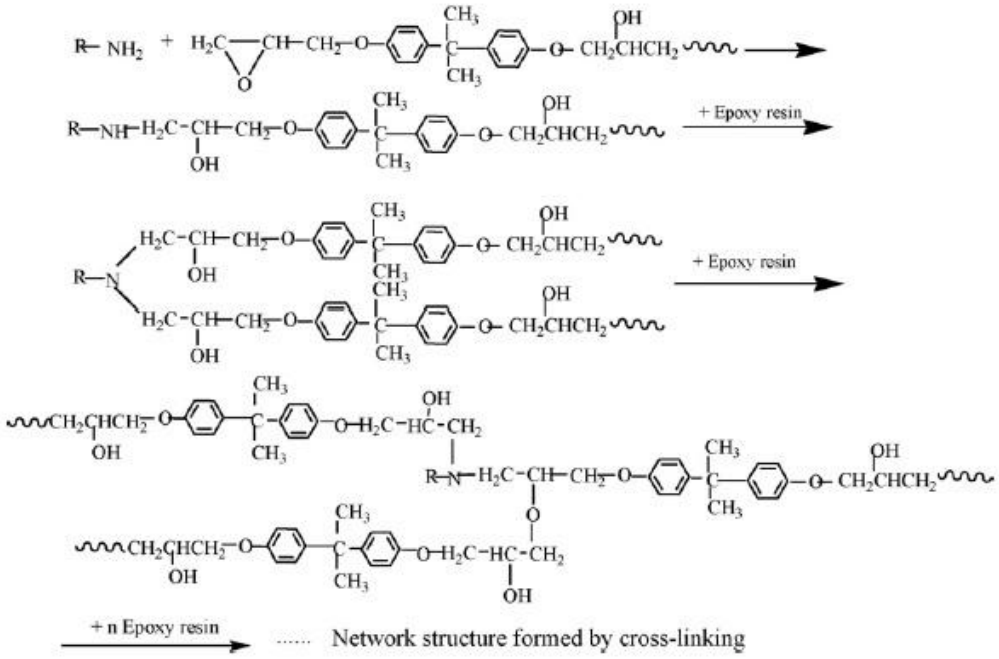

Figure 2.1: Curing Reaction of Epoxy (Luo, Li, & Lan, 2007)

2.2 Carbon Black (CB)

There are more than 40 grades of CB available in market and being use in polymer industry. The properties and grades of carbon black are categories by its structure, surface area and condition. Recently, a system for the designation of CB types was invented by the production and consumer industries which used the initial letters of words that describe a particular CB. I.e.: SAF is stand for Superabrasion furnace black and HAF is stand for High-abrasion furnace black. This method is replacing the technical classification system developed by the American Society for Testing and Materials (ASTM) which adopted in 1966. The system is originally for rubber-grade carbon and consists of a letter followed by a three-digit number. The letter N stands for normal cure of a rubber compound and the first digit are represent the group number which is determined by the average primary particle size as measured by electron microscopy. The particle range of carbon black is divided into 10 groups which show in Table 2.1. The second and third number of this system are numbers that are assigned arbitrarily. I.e.: HAF has ASTM number N110 which mean its particle size is in the range of 0-10 nm (ASTM International , 2005a).

Table 2.1: Particle Range of Rubber-grade Carbon Blacks (Auchter, 2005)

Group number	Typical average primary particle size (nm)	Average surface area (m^2/g)
0	0-10	>150
1	11-19	121-150
2	20-25	110-120
3	26-30	70-99
4	31-39	50-69
5	40-48	40-49
6	49-60	33-39
7	61-100	21-32
8	101-200	11-20
9	201-500	0-10

CB contributes in polymer industries by improving tensile strength, resistance to abrasion, thermal resistance, electric conductivity, and others properties of polymer. Table 2.2 listed out some of the major types of CB with the production data, specification and usage of it. Commercial modifications on CB have been made for matching the requirement of market; for example, one producer alone lists five different grades of ISAF carbon black, including low degree of aggregation, low modulus, high degree of aggregation and others (Auchter, 2005).

Table 2.2: Grades, Properties and Uses of Carbon Blacks (Auchter, 2005; Dannenberg, 1978; Lyon & Burgess, 1985)

Type	Designation		Production process and/or feedstock	Average primary particle diameter (nm)	Iodine absorption number* (g/kg)	Primary rubber processing properties and use
	Acronym	ASTM				
Superabrasion furnace black	SAF	N110	Oil Furnace	17	145	High reinforcement; used in special and off-road tyre products for which require high abrasion resistance.
Intermediate superabrasion furnace black	ISAF	N220	Oil Furnace	21	121	High reinforcement and tear strength, good processing; used in passenger, off-road and good abrasion resistance special tyres.
High-abrasion furnace black	HAF	N330	Oil Furnace	31	82	Medium-high reinforcement, low modulus, good flex, tear and fatigue resistance; used in tyre tread, carcass and sidewall compounds, motor mounts, weather-stripping and bicycle tyres.
Fast-extruding furnace black	FF	N550	Oil Furnace	53	43	Medium-high reinforcement, high modulus and hardness, low die swell and smooth extrusion; used in tyre inner liners, carcass and sidewall compounds and hose and other extruded goods.
General-purpose furnace black	GPF	N660	Oil Furnace	63	36	Medium reinforcement and modulus, good flex and fatigue resistance, low heat build-up; used in tyre carcass, inner liners and sidewalls, sealing rings, cable jackets, hose and extruded goods.
Semi-reinforcing furnace black	SRF	N762	Oil Furnace	110	27	Medium reinforcement, high elongation and resilience, low compression set; used in mechanical goods, footwear, inner tubes and floor mats
Medium thermal black	MT	N990	Natural gas	320	9	Low reinforcement, low modulus, hardness, hysteresis and tensile strength, high elongation and loading capacity; used in wire jackets, mechanical goods, footwear, belts, hose, gaskets and tyre inner liners.

2.3 Morphology

Morphology of epoxy can be determined by Fourier transform infrared spectrometer (FTIR). The absorption peak at 1250, 913 and 830 cm^{-1} are results from the stretching vibrations of epoxide groups. A strong peak at 1510 cm^{-1} is ascribed to the –C–O–C– vibration absorption of a phenyl ring. These absorption peaks are weakened even disappeared after epoxy resins were cured with ethylenediamine, diethylenetriamine and triehytlenetetramine. A weak vibration occurred at 1649 cm^{-1} which is suspected to be the –NH– stretching mode of cured resultants. The FTIR data preliminarily confirmed that the cured reaction might be happen mainly between epoxy groups and the amidocyanogen $–NH^2$. The C=C stretching vibration of a phenyl ring show an absorption peak at about 1610 cm^{-1}. A wide stretching vibration at range 3200-3600 cm^{-1} is results by the hydroxyl group –OH band of epoxy resins. The absorption peak occur at 3400 cm^{-1} is results of the combined stretching bands of the –OH and –NH groups formed by the curing process, which shows the functional group and reaction of the cured process. This is in agreement with the cured mechanism of primary aliphatic amine curing agents and epoxy resins (Luo et al., 2007).

The term epoxy equivalent (epoxy equivalent weight) is defined as the weight of resin in grams, which contains once equivalent gram of epoxy. Epoxy index was calculated to be 5.2-5.4 equiv./kg and epoxy equivalent weight was 85-192 g/equiv. from the research, we can find that the methyl groups ($–CH^3$) of (2,2'-Isopropylidenne (bisphenol A) are showing a vibration at 1382.8 cm^{-1} and the presence of methylene ($–CH^2–$) shows a absorption peak at 1450 cm^{-1} which moieties of epichlorohydrine. The vibration peak of 827.4 cm^{-1} indicates the presents of aromatic hydrogens. The peak at 3300 cm^{-1} is found to be bending vibration of hydroxyl group, which is correlated to the interaction between amine as curing agent and hydroxyl group of epichlorohydrine. The appearance of absorption band at 1249 cm^{-1} is represent alkyl aryl ether which is an interaction between bisphenol A and epichlorohydrine. Vibration at 1033.7 cm^{-1} is ascribed to dialkyl ether which is the cross-linking reaction. The peak at 1182.2 cm^{-1} represent the C–N stretching shows the reaction of secondary amine (piperidine) with epoxy group. Epoxy resin blend with ENP nanoparticles was recognise by a band at 1735 cm^{-1} which involve the

vibration of the carbonyl group of the esteric functionalities in the ENP structure. The =C–H bending vibration are 698.1 and 753 cm^{-1}. The aliphatic C–H vibration at 2874 cm^{-1} proves the existing of aliphatic moieties (Khoee & Hassani, 2010).

Besides the FTIR, scanning electron microscopy (SEM) is always used to determine the dispersion rate of filler and structure of polymer. The CB particles will exist in the form of aggregates in the epoxy system (Etika, Liu, Hess, & Grunlan, 2009). Those particles tend to disperse randomly in the epoxy system and well connected with each other. The distance between those individual clusters and aggregates are large and the space between them is filled with polymer. There are no obvious fractures are observed at lower concentration of filler; when concentration is high fractures are significant which indicate increase in the filler content facilitates the generation of fractures (Zhang, Blackburn, & Dehghani-Sanij, 2007).

2.4 Microstructure Characterization

The microstructure of epoxy can be elucidated by using X-ray diffraction (XRD) machine. Diffraction peak shift might occur with additional of fillers. The sharp Braggs peaks show the samples still remain in intercalated structure after melt-mixing with fillers (Wu, Wu, Zhang, & Wu, 2007). The secondary diffraction peak is weakened or even disappears with increasing of fillers. We can suspect that the samples with exist of secondary may present a well ordered intercalated structure (highly crystalline).

In the case of AEAPTS-MMT/epoxy nanocomposites, no diviation of firraction peaks at low angles for the samples containing filler lower than 2.5 wt.% which shows that the silicate layers are exfoliated. However, for sample containing 5 wt.% of silylated clay shows a small and broad peak around 5.0 °with a d spacing of 1.7 nm. The peak is appeared at the same region as the pure sililated clay indicating that the clay is not exfoliated at this concentration. Apart from that, broadening of the peak indicates the system of epoxy is disordered. X-ray diffraction unable to provide adequate information about the dispersion of filler in epoxy matrix because it is

sensitive to the volume fraction of crystalline phase present in the sample. If the volume fraction of crystalline phase is low in the sample, the corresponding peak or phases will not be displayed in the XRD pattern (Silva, Dahmouche, & Soared, 2011).

2.5 Rheology

2.5.1 Effect of Volume Fraction of Filler on Viscosity

Besides filler size, rheological properties of polymer were also affected by volume fraction of filler. Filler content is usually specified by weight percentage (wt.%). Using wt.% in scale is convenient for measurement, but it is the volume occupied by the filler that determines the ultimate viscosity (Bullard, Pauli, Garboczi, & Martys, 2009). In simple, the viscosity of a disperse system increase as the volume fraction of the suspended filler increase. But the increment of viscosity is not noticeable with small amount of filler. From studies, viscosity of epoxy is not much change with the filler load increase in the range of 0.2 to 0.6 volume fraction. The viscosity shows a sharp increase at a filler content of 0.8 volume fraction. With increasing of concentration of the filler, the particle-particle interactions increase weakly at first and become stronger as the concentration becomes higher and higher. The concentration at which inter-particle interactions begin depends on the contact surface area and collision between the filler particles. At volume fraction 0.8, the concentrations of filler are enough to have a closer contact, resulting in a higher degree of fillers agglomeration (Irfan & Kumar, 2008).

With finding of Etika et al. (2009), under room temperature (25 ℃) storage moduli of the composites increase with the increase of CB concentration. Samples with 2.5 wt.% and 5 wt.% CB show 19 % and 23 % higher modulus than neat epoxy. For sample containing 0.5 wt. % clay, no significant improvement in storage modulus but equal amount of CB and clay composites increased the modulus by 36 %, 40 % for 2.5 wt.% and 5 wt.% CB filled epoxy, respectively. By adding equal amount of clay and CB results in doubling the total additive concentration and the

increment in storage modulus could be the results of this. Sample with clay:CB ratio of 1:1 exhibited 11 % and 15 % increases in storage modulus relative to composites containing CB or clay alone, respectively. The research suggested an interaction between clay and CB can lead to better dispersion of CB and clay in the presence of one another. It is known that the composites containing more uniformly dispersed filler will have higher storage moduli value.

From another study, surface of the neat epoxy polymer do not appear matrix tearing. Micro-cracks are observed around the carbonized particles region in the matrix. The carbonized materials (CB) were acted as stress concentrators if added into epoxy system. In addition, concentration of filler further promoted the formation of star-like cracks. So, it is believed that, with the increase of CB might increase the flexibility and mechanical properties of the epoxy (Abdul Khalil, Firoozian, Bakare, Md. Akil, & Md. Noor, 2010).

2.5.2 Effect of filler size on viscosity

By Durairaj et al. (2010), higher weight percentage of smaller particles results in more inter-particle interaction and increase the resistance to flow. When shear rate increased, this effect will become less marked. It is due to the inter-particle interaction are relatively weak and broken down at high shear stress rate. At zero shear rate the viscosity of isotropic conductive adhesives (ICAs) with the silver flakes filler has the highest viscosity. The smaller filler particles have larger surface area. It increases the contact between particle in ICAs and form bond more easily. With more interaction between particles, viscosity of ICAs with smaller filler particles will be higher than that with larger filler particles. The results show that as the particle size (10 μm for silver flakes and 250 μm for silver powder) of filler decreases, the viscosity increase. Smaller particle size filler tends to disperse better in the flux system.

In addition, the filler particles tend to agglomerate in to larger flocs in the system. This condition increase the resistance of flow of the ICAs and viscosity is

being increased. With the same idea, large particle size (low specific surface area) filler has lower contact surface causing poor dispersion ability which leads to lower viscosity. So it can be concluded that, CB with larger surface area (smaller size) will provide higher viscosity in the CB-epoxy blend. Besides that, the viscosity of epoxy also decreases along with the increasing of temperature (Tao, Yang, Ge, Chen, & Fan, 2006).

2.5.3 Effect of Filler on Viscoelastic Behaviour

In typical rheology experiment, storage modulus (G') and loss modulus (G") are always being measured. At lower frequency, the hydrogel particles response as viscous-like where the loss modulus is much higher than storage modulus. At high frequencies, the response is change to solid-like causing the storage modulus dominates the loss modulus (Wyss, Larsen, & Weitz, 2007). Apart from that, the composites containing more uniformly dispersion of CB will have a higher Storage modulus (Etika et al., 2009). From studies on CB, N550 have a lower particle size compare to CB N774, so N550-epoxy composites is suspected have a higher modulus value.

Particle-filled molten polymer appears in a sol-gel (also name liquid-solid) transition due to the formation of a gel like structure by solid particles additive. This gel character shows by the appearance of a constant elastic modulus at low frequencies corresponding to yield stress behaviours of the viscosity (Elias, Fenouillot, Majeste, & Cassagnau, 2007). When fillers are introduced into epoxy system, fillers is dispersed individually after the destroying of initial aggregates. The filler is percolate in three-dimensional network which cause the solid-like behaviour of the epoxy. However, the matrix structure are not strong enough to resisting the increase of strain and broken. The solid-like behaviour of epoxy degraded into liquid-like material (Franchini, Jocelyne, & Gérard, 2009). The phase change is name as shear thinning and matrix structure of the pastes was undergoing changes due to destruction of flocculation in the systems (Bao, Lee, Raj, Rangen, & Maria, 1998).

CHAPTER 3

METHODOLOGY

3.1 Materials

The epoxy used were Jotafloor Coating- Compound A and Jotafloor Coating - Compound B(20) as the cross linking agent were provided by E.P.P. Flooring System Sdn. Bhd and was used as received. The composition of epoxy and curing agent is listed at Table 3.1 and 3.2. Carbon black N550 and N774 were purchased from Technochem Trading and their performance parameters are shown in Table 3.3.

Table 3.1: Composition of Jotafloor Coating– Compound A

Name	Percentage (%)
Bisphenol-A-(epichlorohydrin)	50-100
Oxirane	20-25
Poly[oxy(methyl-1,2-ethanediyl)]	2.5-10
Solvent naphtha (petroleum)	0-1
Stoddard solvent	0-1
n-methyl-2-pyrrolidone	0-1

Table 3.2: Composition of Jotafloor Coating– Compound B (20)

Name	Percentage (%)
3-aminomethyl-3,5,6-trimethylcyclohexylamine	25-50
Benzyl alcohol	25-50
Salicylic acid	2.5-10
2,4,5-tris(dimethylaminomethyl)phenol	2.5-10

Table 3.3: Specification of Carbon Black (CB)

Type	Diameter (nm)	Supplier
N550	53	Technochem Trading
N774	110	Technochem Trading

3.2 Composite Preparation

CB N550 and N774 were dried in vacuum at 50 ℃ for 48 h before added into the epoxy resin. The additives shown in Table 3.4 were added into the epoxy resin at room temperature and stirred for 5 minutes. After completely mix, the curing agent were added to the above mixture under vigorous stirring with specific ratio. The compound was cured in a petri dish for 1 day at room temperature. The cured sheet has a thickness of 3 mm and was cut into proper size for scanning electron microscope (SEM) and X-ray diffraction (XRD) test.

3.3 Formulation

Samples were prepared as the formulation shown in Table 3.4.

Table 3.4: Formulation of Epoxy/Carbon Black Samples

Sample	Ratio (Epoxy resin : Curing Agent)	Carbon black	
		Type	Amount (wt.%)
A	2:1	-	0
B1	2:1	N550	1
B2	2:1	N550	2
B3	2:1	N550	3
B4	2:1	N550	4
B5	2:1	N550	5
C1	2:1	N774	1
C2	2:1	N774	2
C3	2:1	N774	3
C4	2:1	N774	4
C4	2:1	N774	5

3.3 Experiment Technique

3.3.1 Characterization of Morphology

Distribution of CB in epoxy were be observed by Hitachi VP-SEM S-3400N scanning electron microscope (SEM). The cured specimens were cut into 3mm x 3mm square and pasted on a metal pallet for the scan. Particles observed from the SEM were identified with energy-dispersive X-ray spectroscopy (EDX).

3.3.2 Characterization of Microstructure

X-ray diffraction (XRD) studies were performed by X-ray Diffractometer produced by Shimadzu with a model name as LabX XRD-6000. The cured CB-epoxy plate was cut into circular shape to fit in the XRD plate. Scanning speed was set at 2 °per minutes for a range between 10 ° to 80 °. The measurement conditions were fixed at 50 kV for voltage and 30 mA for current.

3.3.3 Measurement of Viscoelastic Properties

Viscosity of samples were obtained by using Physica MCR 301 controlled stress rheometer. Parallel plates geometry was chosen with a diameter of 25 mm. A gap width of 0.7 mm was used. Prior to loading the sample onto the rheometer, the paste will be stirred for about 1-2 min to ensure that the paste structure was consistent with the particles being re-distributed into the paste. A sample was loaded on the peltier plate and the geometry plate was then lowered to the gap of 0.7 mm. The excess sample paste was trimmed off carefully. All tests were conducted at 25 ˚C with the temperature controlled by the Peltier-Plate system. Test parameters were show in Table 3.5 and 3.6.

Table 3.5: Experimental Parameters for Viscosity Test

Experimental values			
Shear rate (s^{-1})	Number of measuring point	Interval between measuring point (s)	Overall Duration (s)
1	20	3	60

Table 3.6: Experimental Parameters for Amplitude Sweep Test

Experimental values				
Strain (%)	Angular frequency (s^{-1})	Number of measuring point	Interval between measuring point (s)	Overall Duration (s)
0.001-100	10	20	3	60

CHAPTER 4

RESULTS AND DISCUSSION

4.1 Morphology Characterization

4.1.1 Dispersion of Carbon Black in Carbon Black-Epoxy Composites

The dispersion state of filler and its matrix structure in polymer interfacial interaction are two important factors influencing the properties of those composites (Wen et al., 2012). Figure 4.1 shows the SEM image of neat epoxy resin. The small amount of white dots in the epoxy are due to air bubble contain in epoxy. The dispersion morphology of CB in epoxy is clearly shows in Figure 4.2. The black colour area is the epoxy while the white particles within the epoxy are carbon black. The larger magnification of SEM image provided in next section proved the present of carbon black particles in epoxy resin.

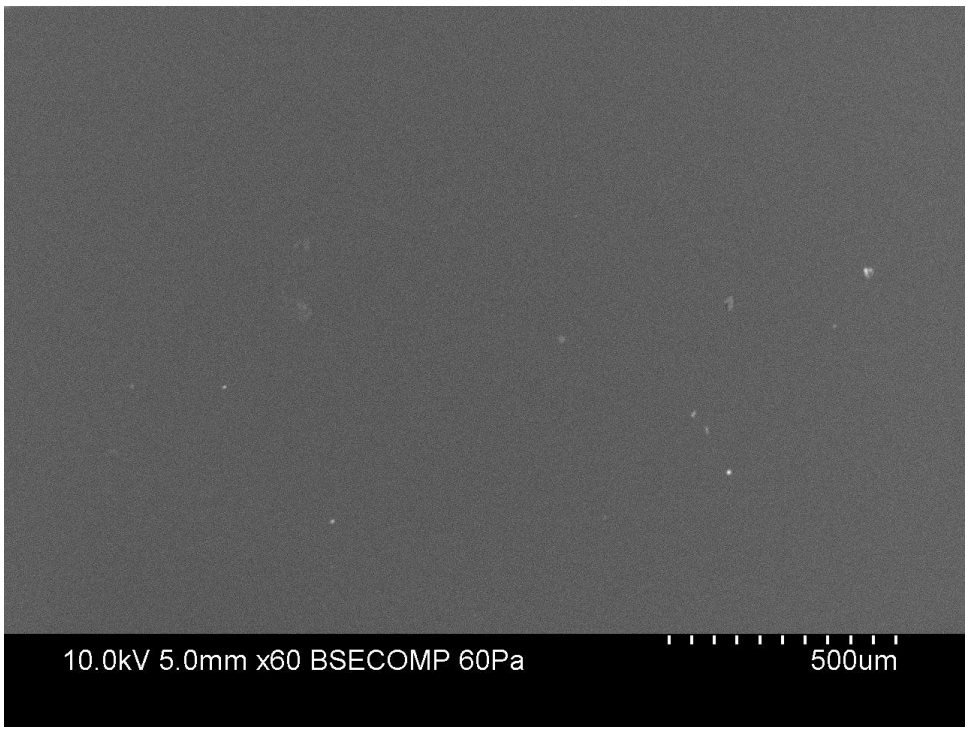

Figure 4.1: SEM Image of Neat Cured Epoxy

The dispersion of CB is greatly depending on concentration of CB. With the increasing of wt.% of CB particle, the density of white particles in epoxy are increased. The CB particles are distributed randomly between the epoxy and function as enhancement particles. Due to the samples which were prepared by hand mixing, the distribution of CB was not uniform as in Figure 4.2 (a) and 4.3 (a). It was observed that, when concentration of CB was low, there were no obvious CB aggregates composites to be observed. When the CB content was high, large particles start to appear and the increase of CB concentration increase possibility generation of CB aggregates. The large surface area CB (N550) tends to form aggregates more positively as we can compare the results from Figure 4.2, 4.3, 4.4, 4.5 and 4.6. The CB particles form aggregates and agglomerates were distributed uniformly in the samples, but the distances between individual clusters were relatively large and the space between them was filled with epoxy (Zhang et al., 2007; Wen et al., 2012).

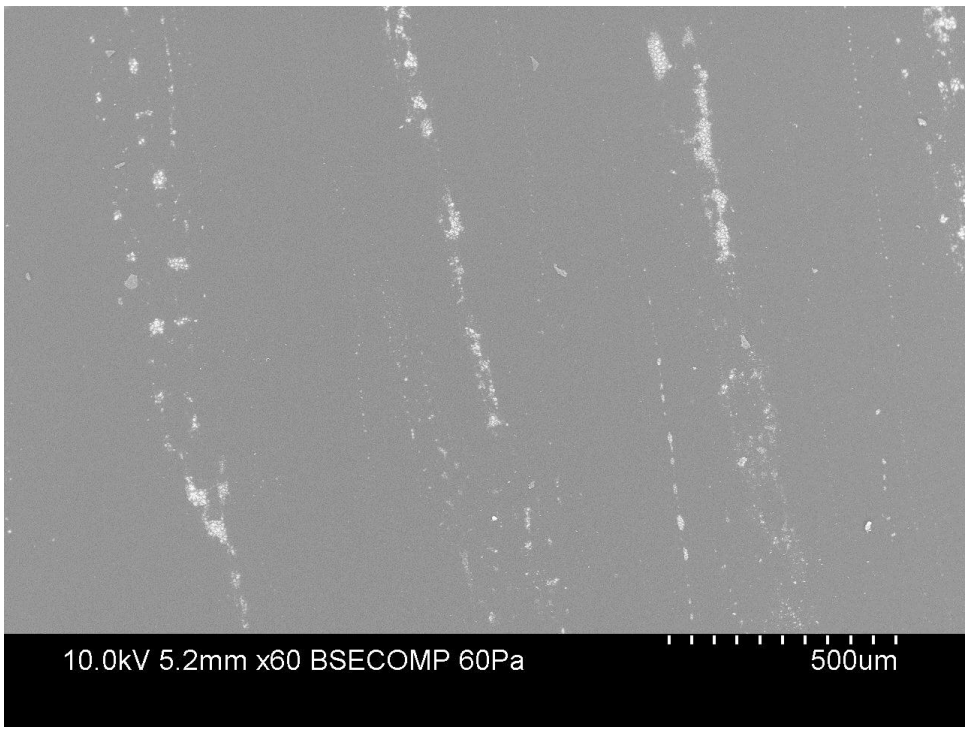

(a)

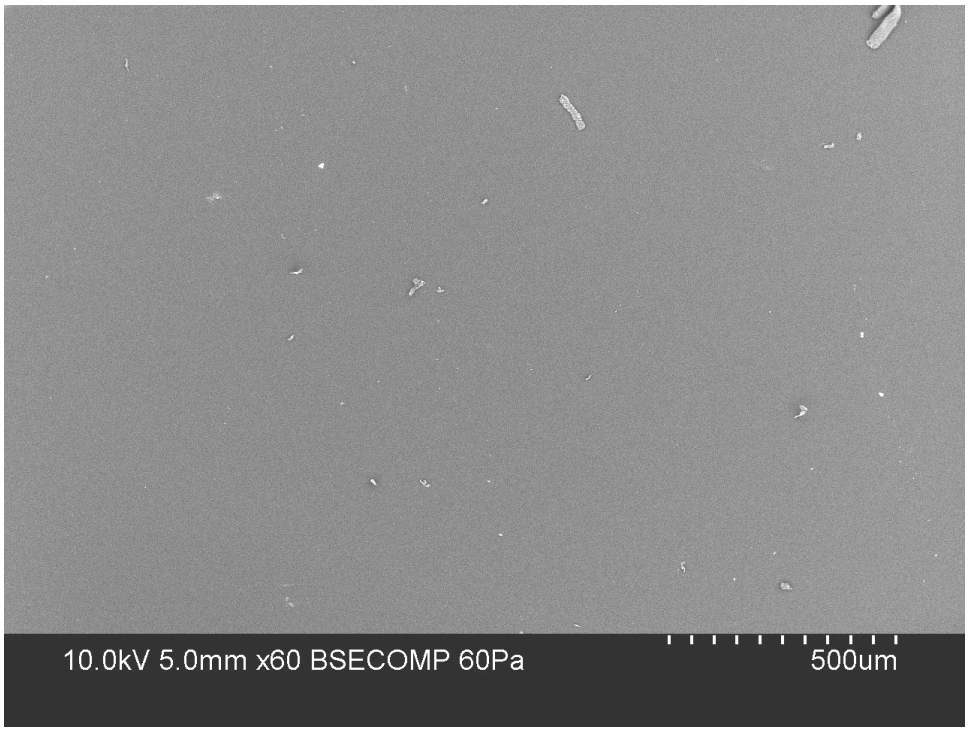

(b)

Figure 4.2: SEM Images of Carbon Black Distribution in Cured CB-Epoxy Composite with (a) 1 wt.% of CB N550 and (b) 1 wt.% of CB N774

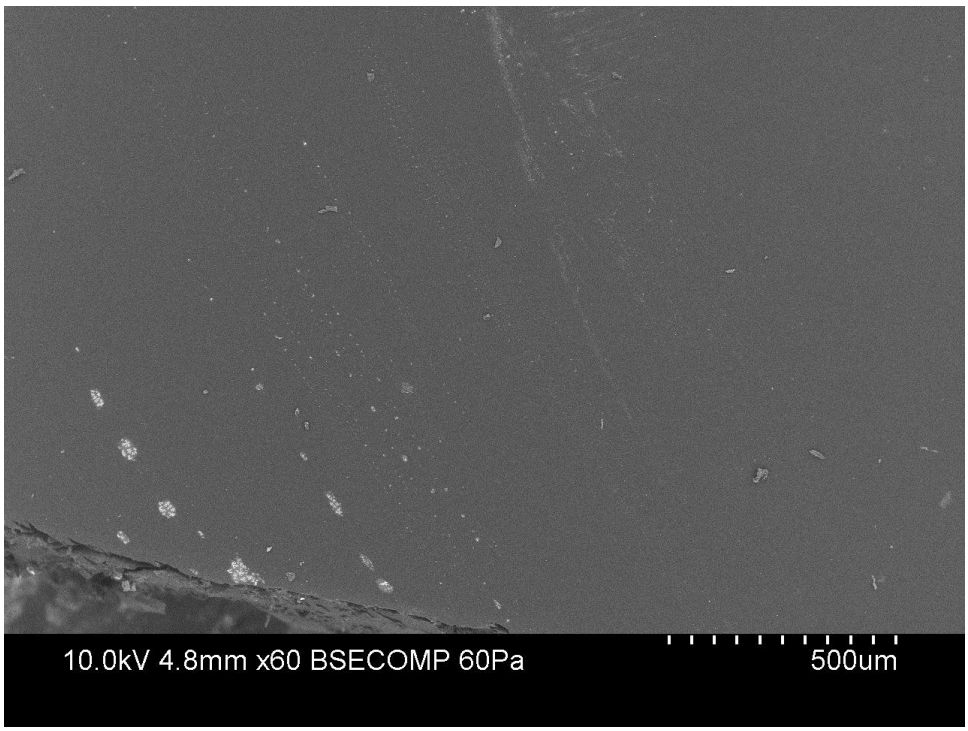

(a)

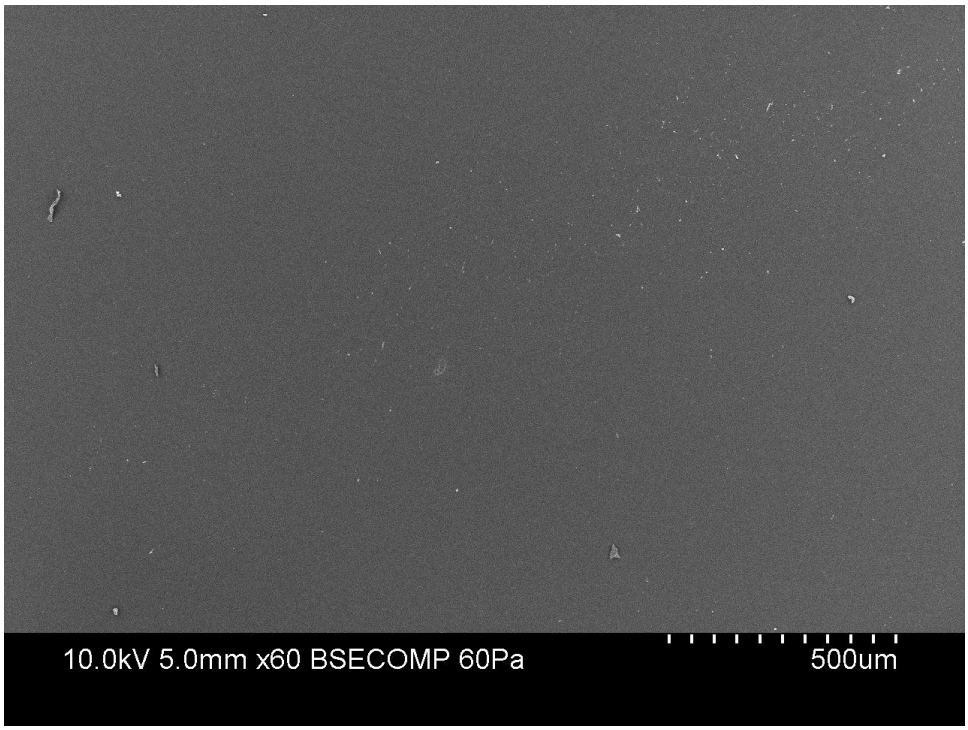

(b)

Figure 4.3: SEM Images of Carbon Black Distribution in Cured CB-Epoxy Composite with (a) 2 wt.% of CB N550 and (b) 2 wt.% of CB N774

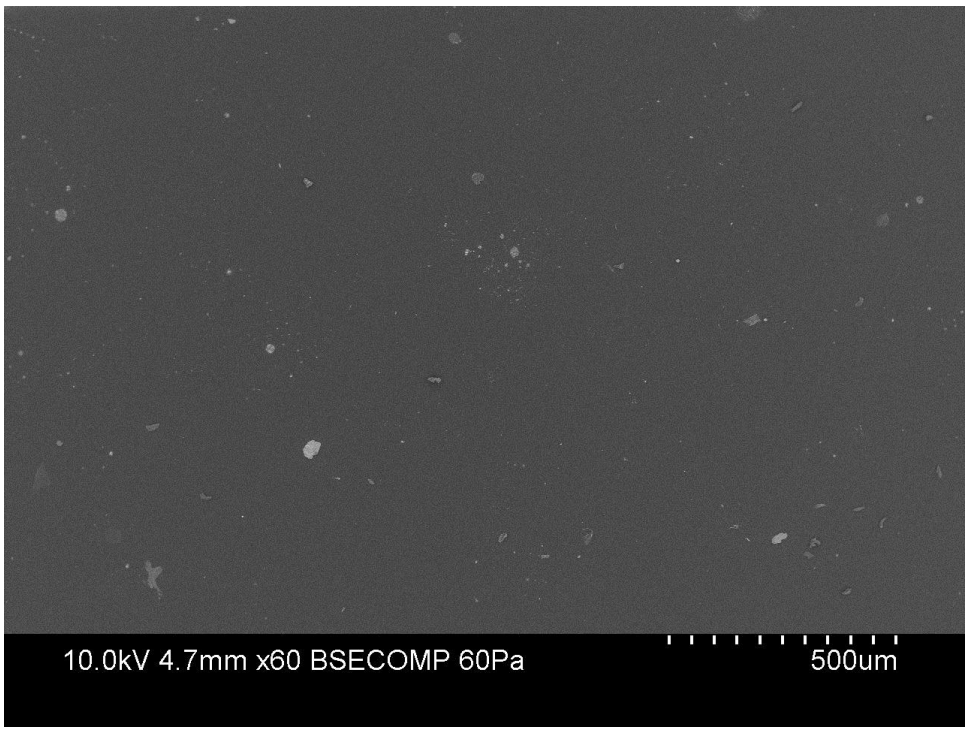

(a)

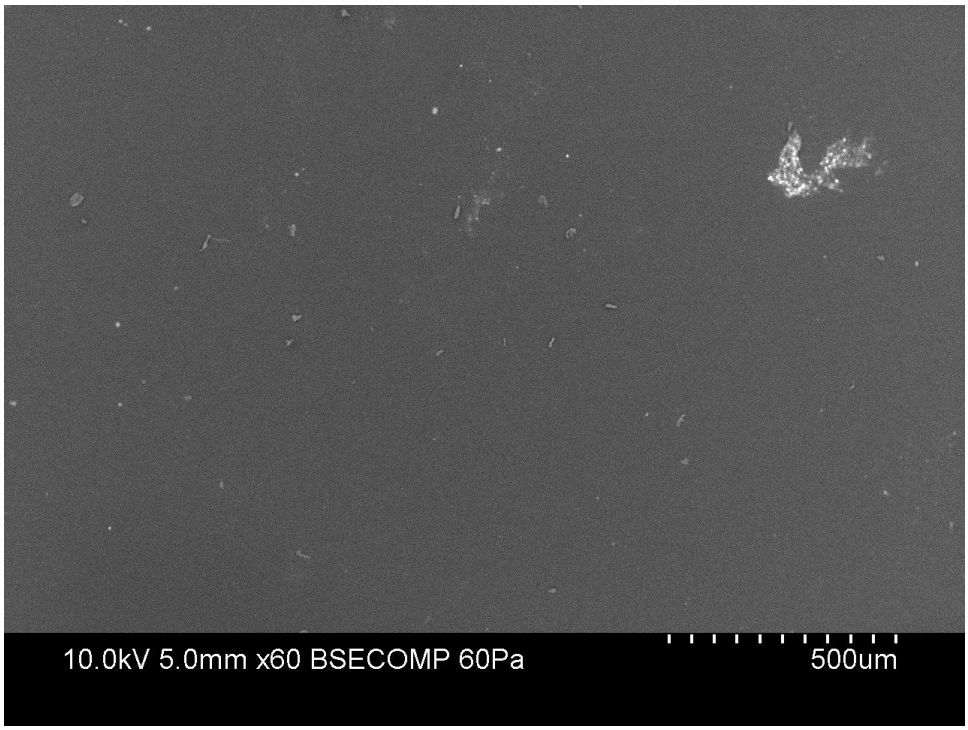

(b)

Figure 4.4: SEM Images of Carbon Black Distribution in Cured CB-Epoxy Composite with (a) 3 wt.% of CB N550 and (b) 3 wt.% of CB N774

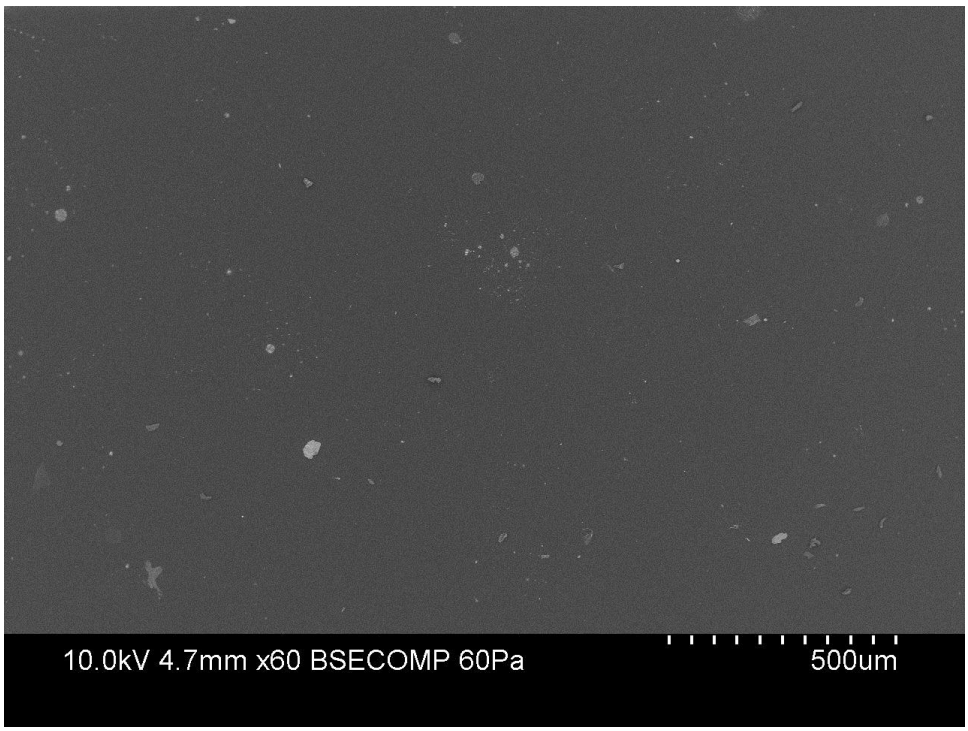

(a)

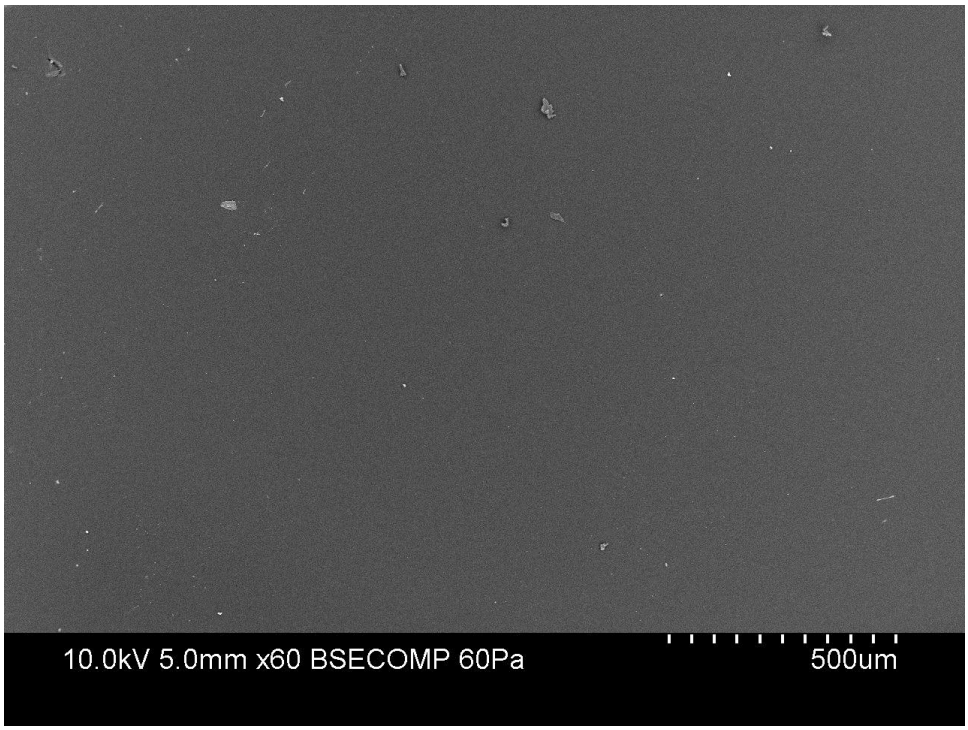

(b)

Figure 4.5: SEM Images of Carbon Black Distribution in Cured CB-Epoxy Composite with (a) 4 wt.% of CB N550 and (b) 4 wt.% of CB N774

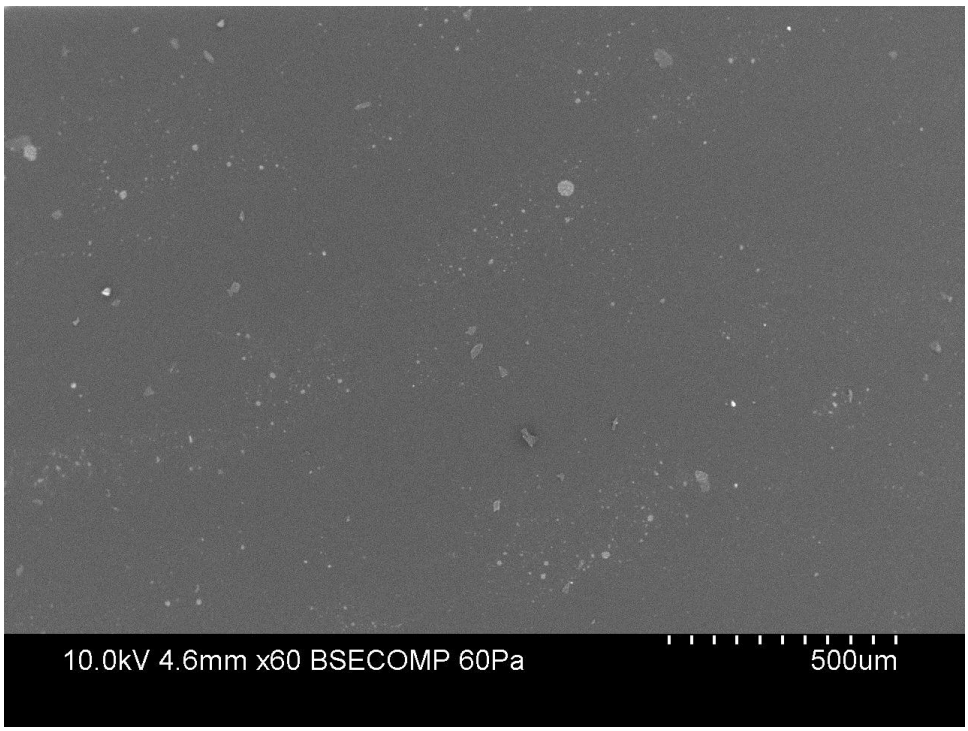

(a)

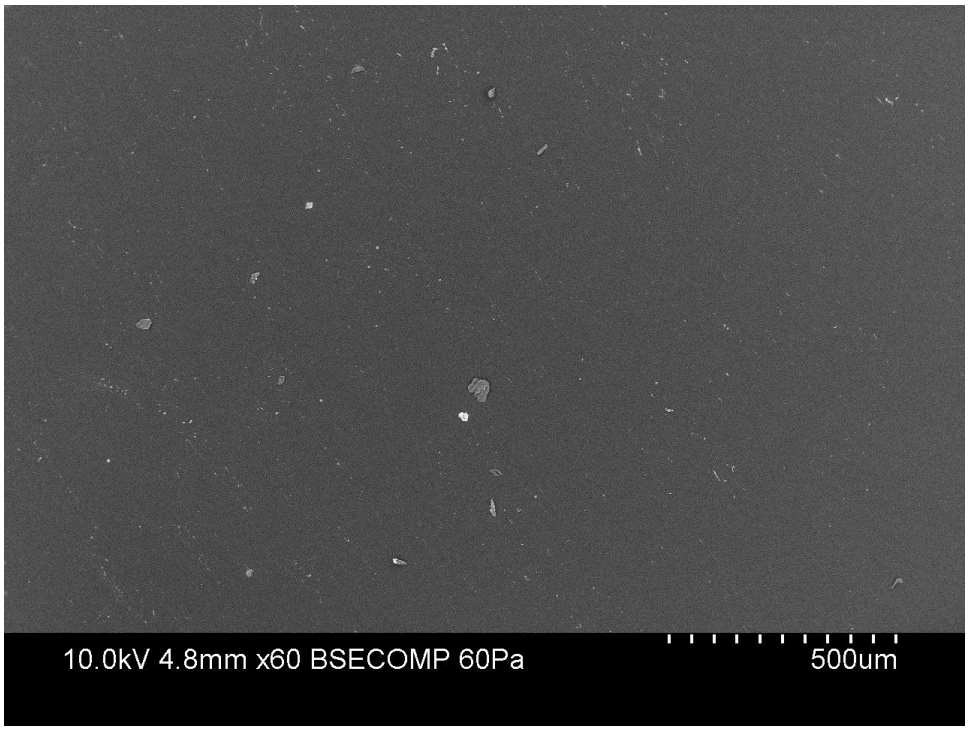

(b)

Figure 4.6: SEM Images of Carbon Black Distribution in Cured CB-Epoxy Composite with (a) 5 wt.% of CB N550 and (b) 5 wt.% of CB N774

4.1.2 Surface Roughness of Carbon Black-Epoxy Composites

Surface morphologies give information about failure process and its mechanism (Kim & Jeong, 2005). Figure 4.7 shows the unmodified sample consist of large-scale roughness and clean surface. With the increasing of CB N774 composition as additive in epoxy resin, the large-scale roughness of epoxy decreased and changed to small-scale roughness surface which is shown Figure 4.8, 4.9, 4.10,4.11 and 4.12. The microstructure of epoxy is affected with the increasing of CB particles. For more details study, stylus type roughness tester and the root-mean-square (RMS) roughness need to be calculated and analysis.

From SEM, micro-cracks were founded in the pure epoxy surface, the CB added in were occupied in those micro-cracks for the CB-epoxy composites. It is believed that increasing additive as CB, it will increase the flexural properties of the CB filled composites (Abdul Khalil et al., 2010). Those CB are suspected functioning as strength adhesive site to allow the CB-epoxy composites have more elastic behaviour compare to pure epoxy which also mean that neat epoxy is less flexible.

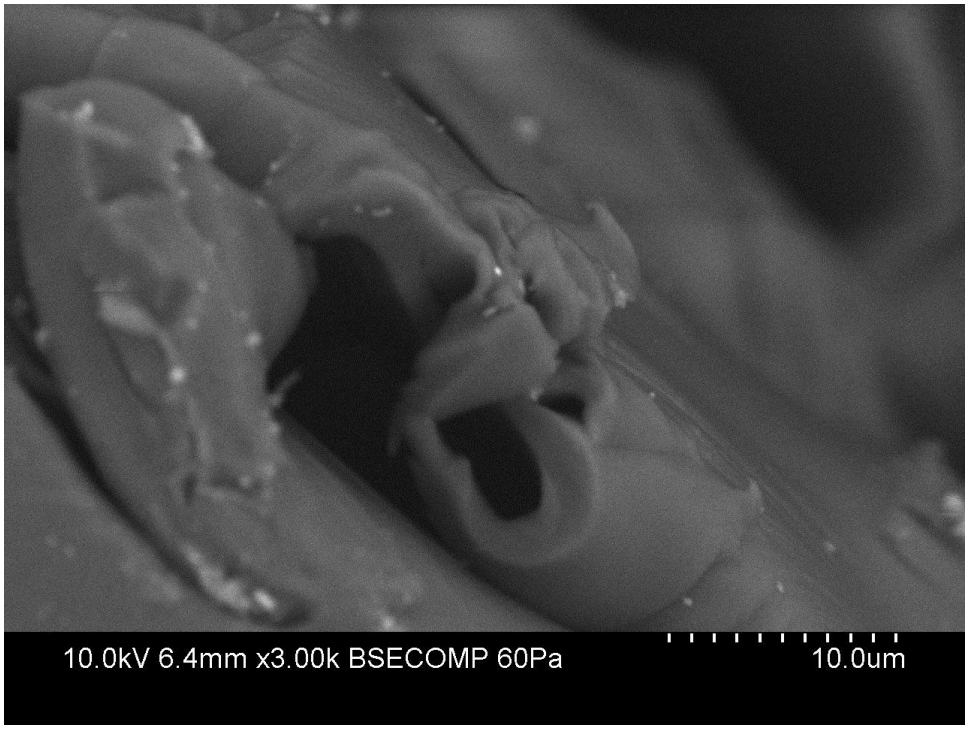

Figure 4.7: SEM Image of Neat Epoxy Surface

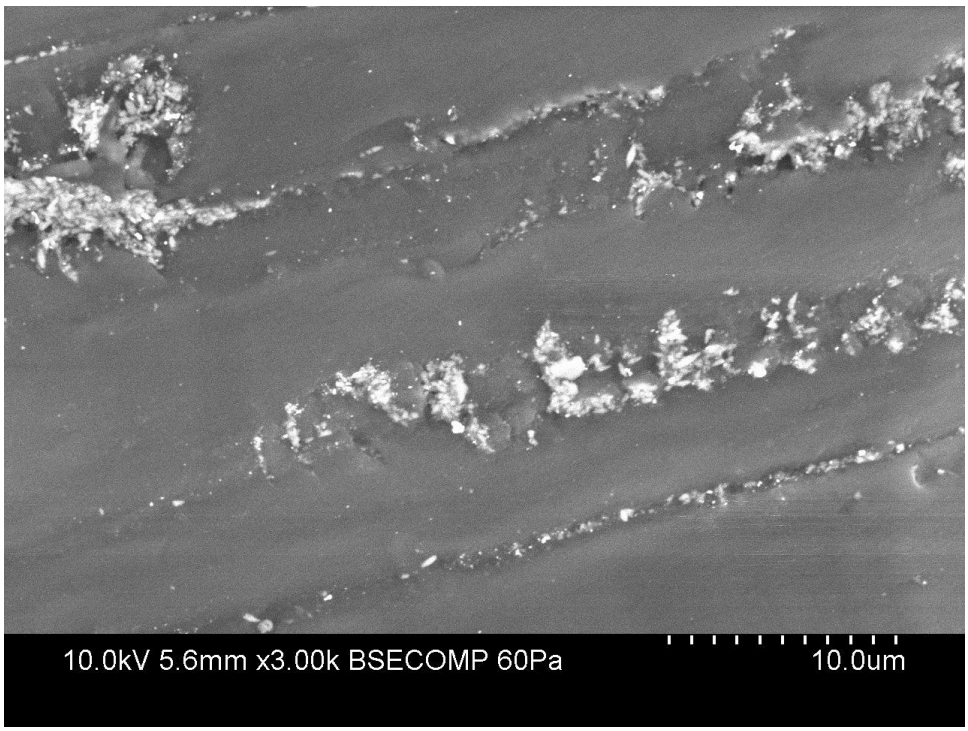

Figure 4.8: SEM Image of 1 wt.% CB N774-Epoxy Surface

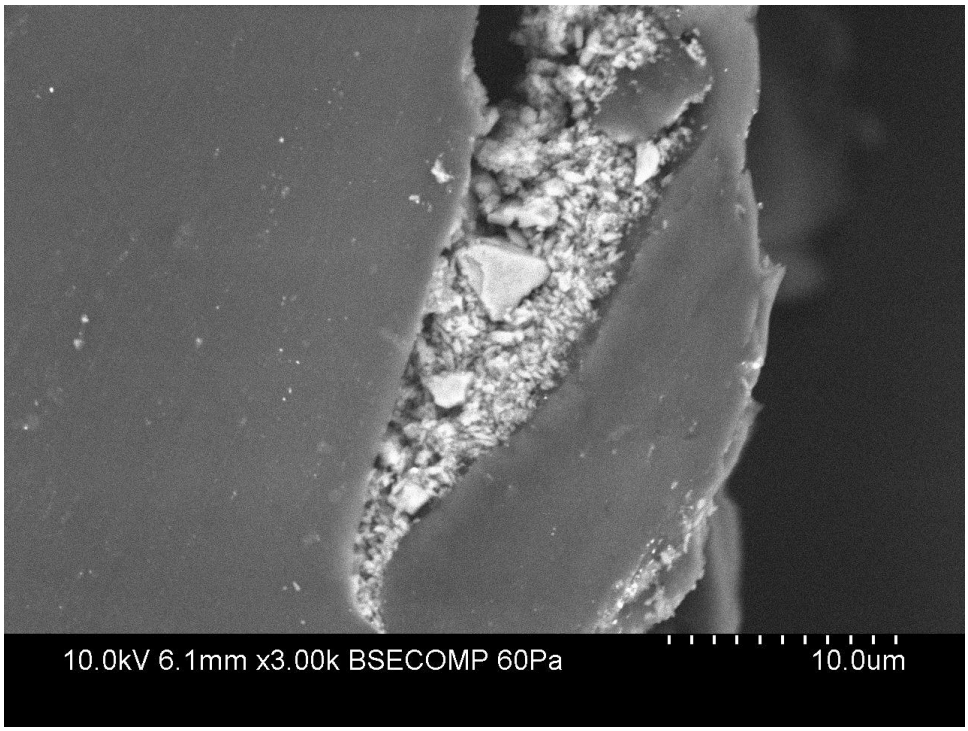

Figure 4.9: SEM Image of 2 wt.% CB N774-Epoxy Surface

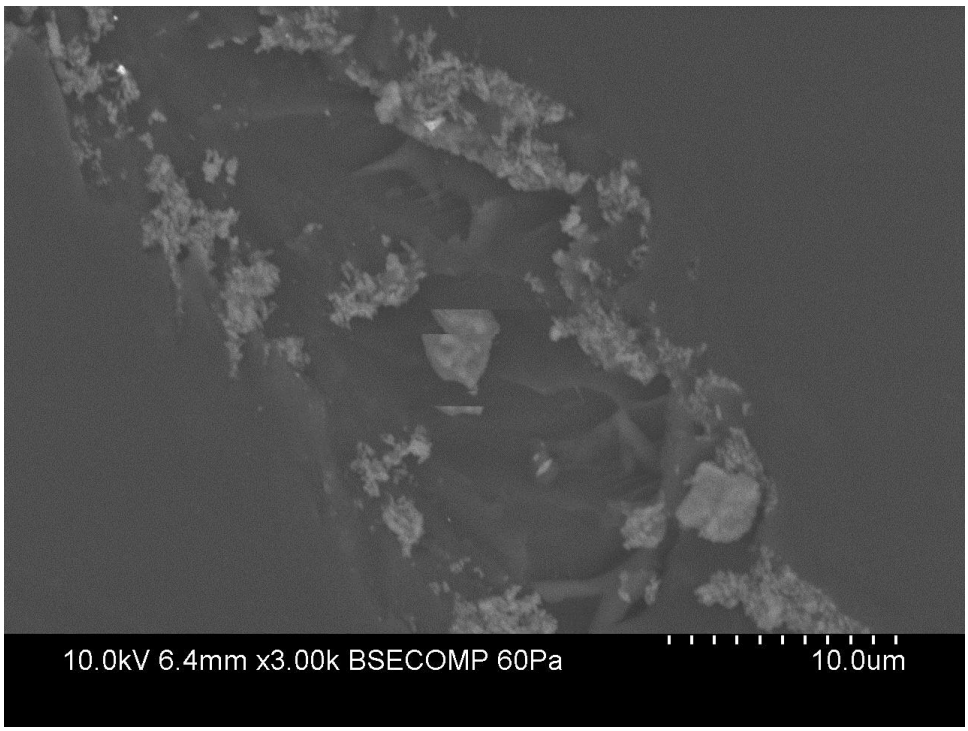

Figure 4.10: SEM Image of 3 wt.% CB N774-Epoxy Surface

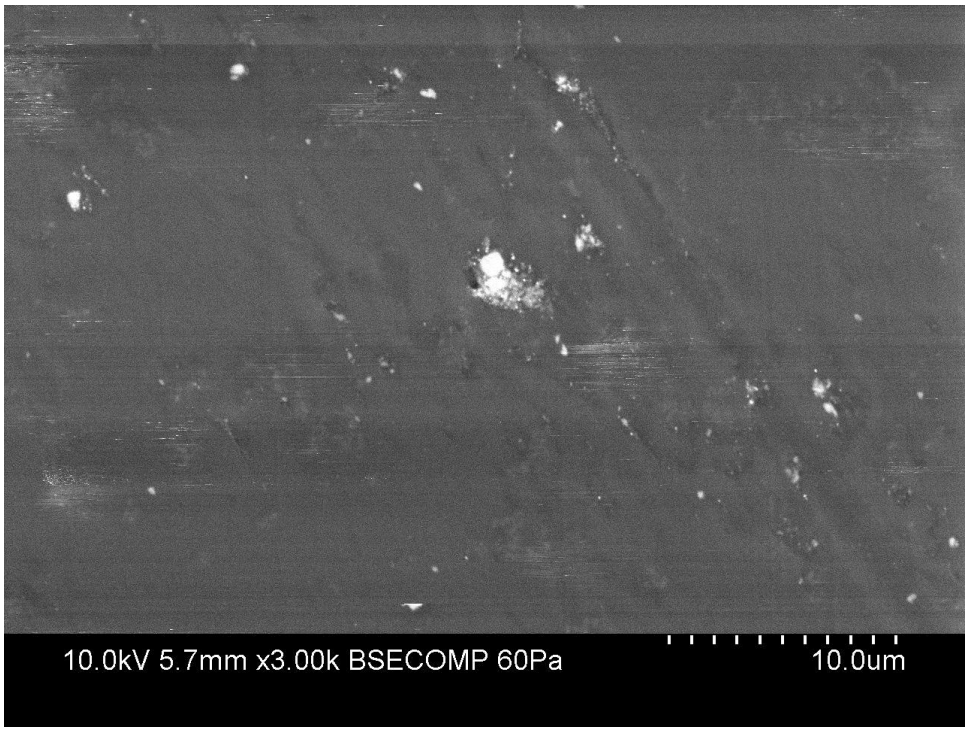

Figure 4.11: SEM Image of 4 wt.% CB N774-Epoxy Surface

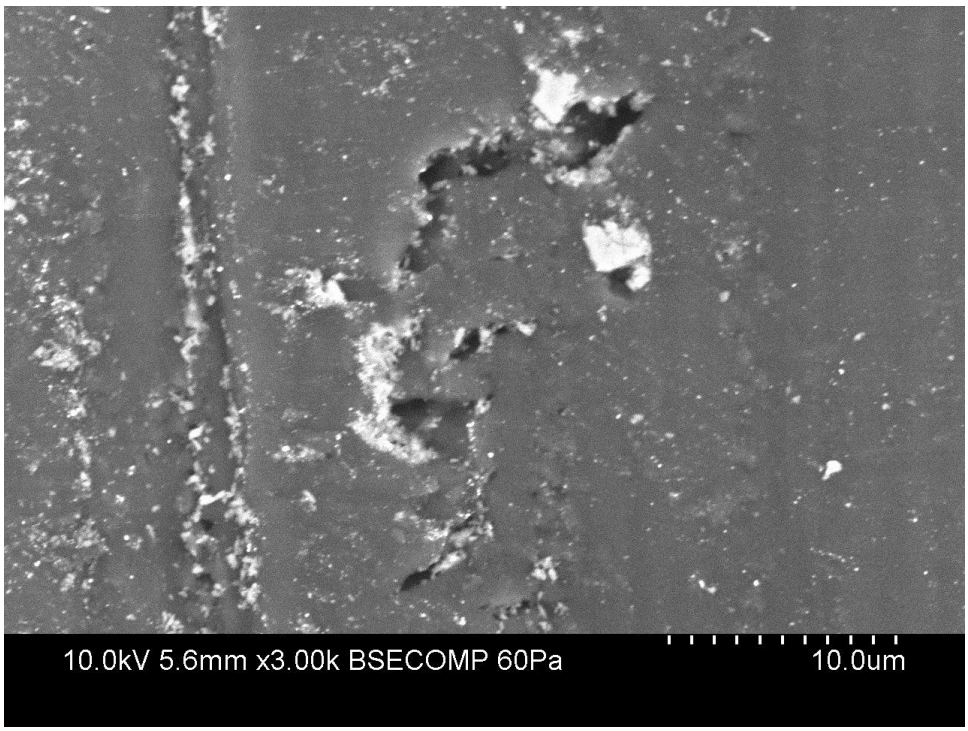

Figure 4.12: SEM Image of 5 wt.% CB N774-Epoxy Surface

4.1.3 Structure of Carbon Black in Carbon Black-Epoxy Composites

Size of the CB N550 is 53 nm while CB N774 is 110 nm (Auchter, 2005). From SEM we found that CB particles tend to form aggregates rather than as a stand-alone particle. CB aggregates with different sizes were randomly distributed in the epoxy matrix with the size mainly in the range of 100-350 nm. As mention at above the size and amount of CB aggregates are increasing with the increase of CB wt.%.

CB N550 aggregates were normally appearing in snow shape as shown in Figure 4.13 but aggregates for CB N774 do not fix in a particular shape as shown in Figure 4.15 (a) and tend occupied in micro crack as shown in Figure 4.15 (b). For CB N550 the snow shape-like aggregates tend to group up and form a bigger circular particle in higher concentration as 5 wt.% shows in Figure 4.14 (b). In 3 wt.% the CB N550 formed a smaller aggregates as in Figure 4.13 or small group of aggregates as shown in Figure 4.14 (a). The studies show that increasing of CB concentration will cause the CB form a larger matrix structure.

It was found that the CB N550 and N774 adhered firmly to the epoxy matrix, indicated a strong interfacial interaction between CB and epoxy chains. This behaviour produces a strong interface adhesion which can turn the large-scale roughness of epoxy surface into small-scale roughness and increase the flexibility of epoxy. But CB N774 tends to act as essentially independent discrete particles compare to CB N550 due to the larger particle size.

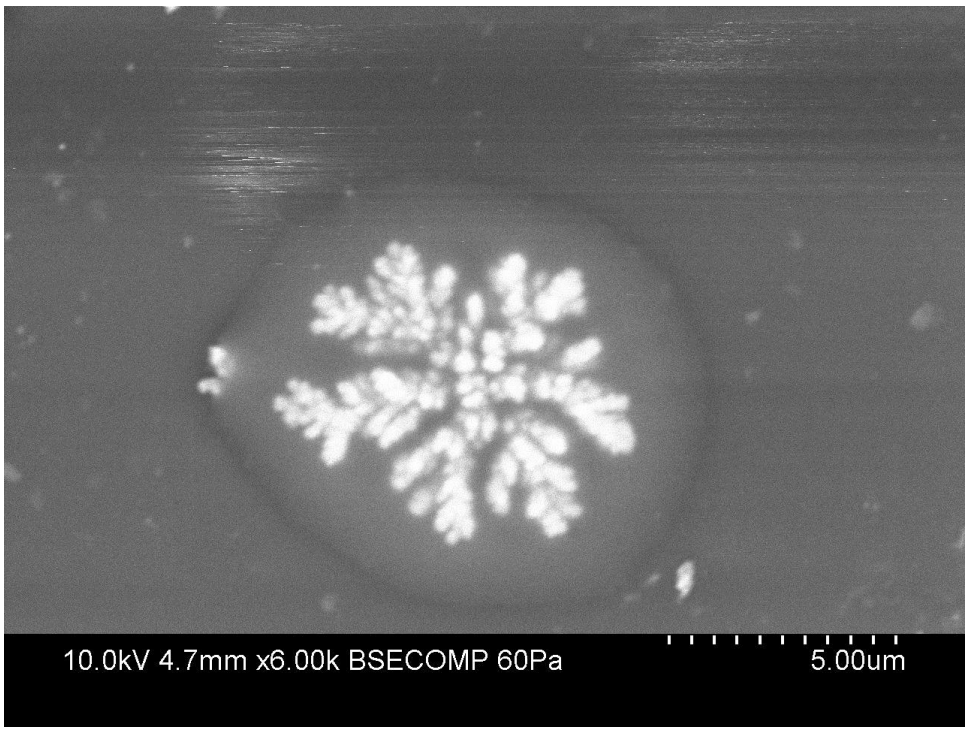

Figure 4.13: SEM Images of Single Carbon Black N550 Aggregate Structure in Cured Epoxy Resin

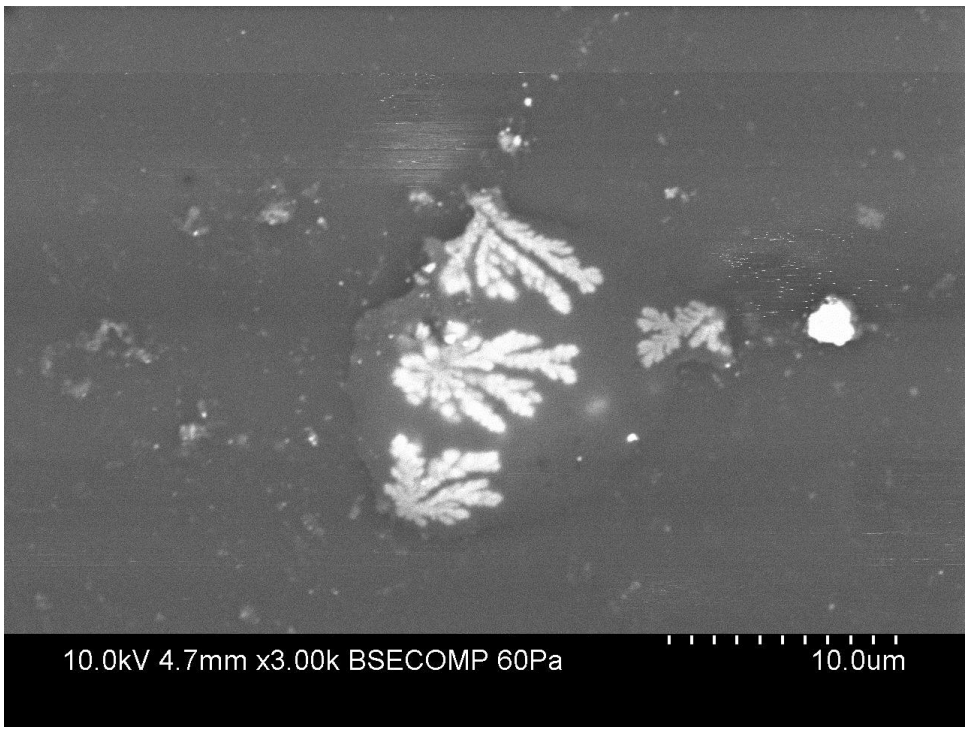

(a)

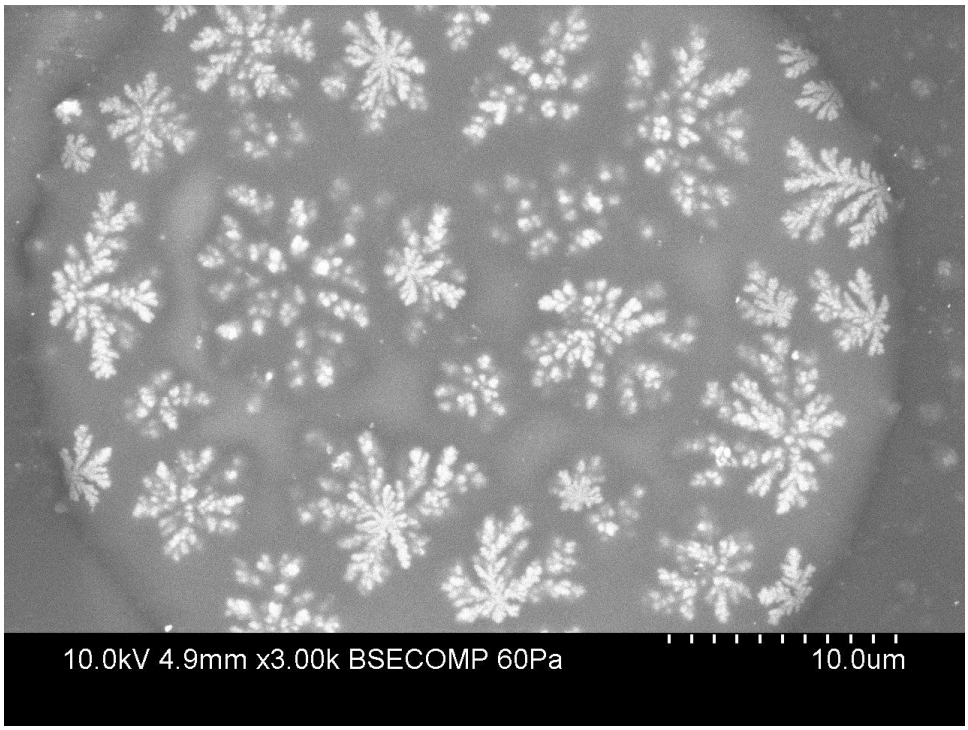

(b)

Figure 4.14: SEM Images of Carbon Black N550 in Cured Epoxy Resin (a) Triple Aggregates Structure (b) Matrix Aggregates Structure

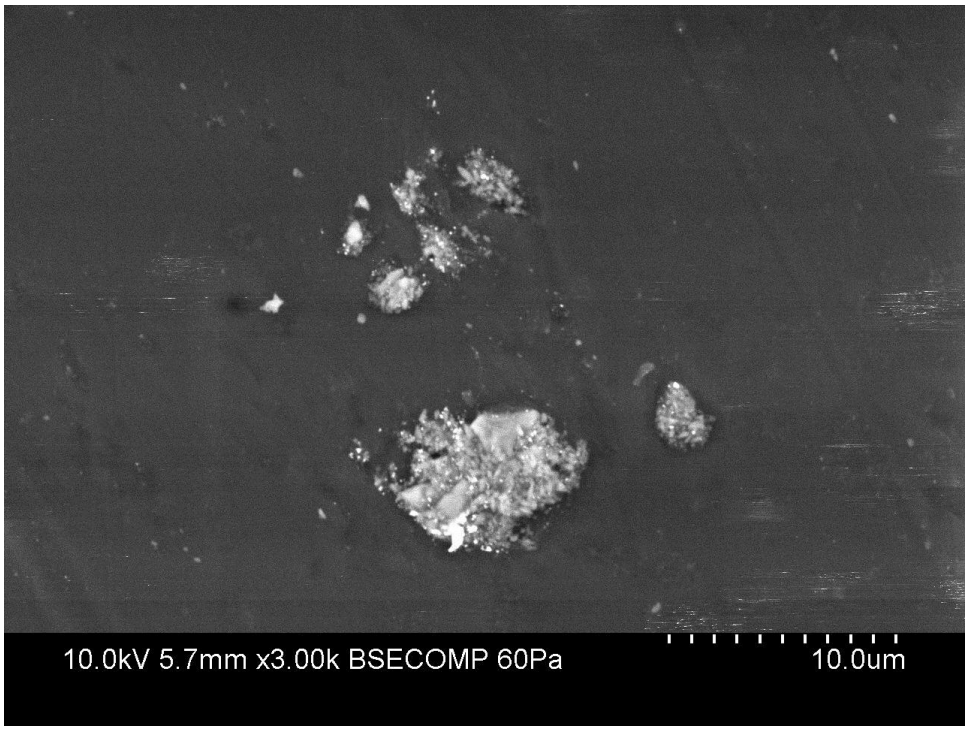

(a)

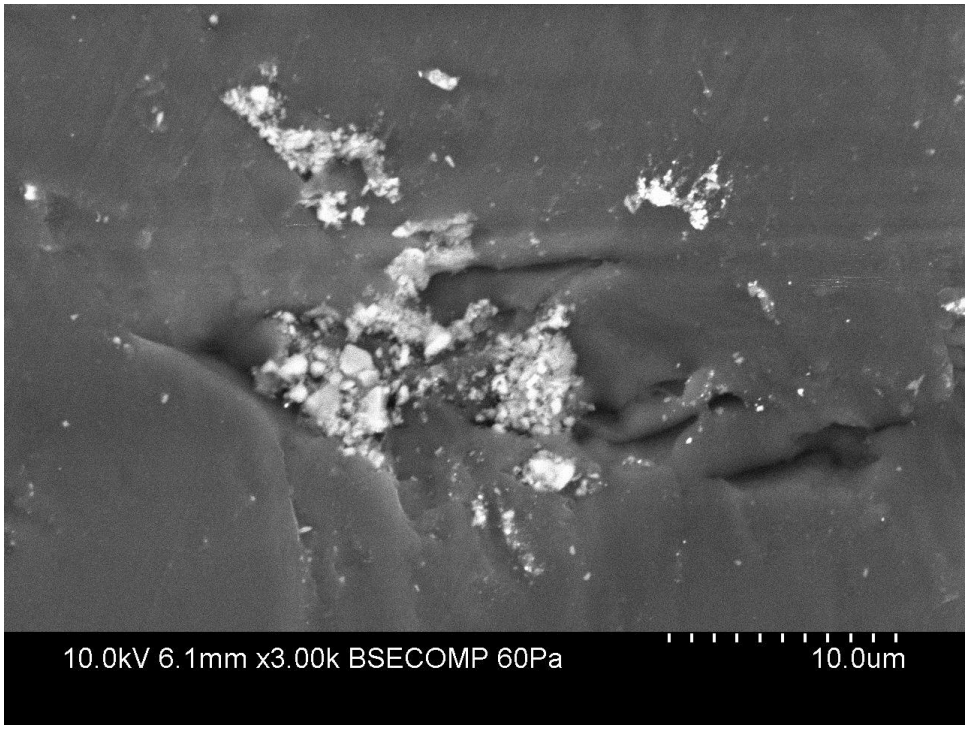

(b)

Figure 4.15: SEM Images of Carbon Black N774 in Cured Epoxy Resin (a) Aggregates Structure (b) Filler in Micro Cracks

4.2 Microstructure Characterization

4.2.1 Effect of Carbon Black on Peak of Epoxy

From the XRD test, X-ray diffraction pattern of CB N550, N774 and neat epoxy were studied and shown in Figure 4.16. The CB N550 and N774 have a similar peak distribution which is located at 24.57 °and 24.81 °. Neat epoxy, located at the lower angle which is 17.36 °. With the addition of CB particles, the diffraction peak shifted higher angles gradually as shown in Figure 4.17 and 4.18 and Table 4.1. The shifting of peak implies some disorder of the epoxy system after introducing of CB (Wu et al., 2007). The peak shifting to higher degree which appeared at the same region as the pure CB N550 and N774 with the increasing of the filler concentration, indicating that the CB is not exfoliated at any formulation of CB-epoxy composites (Silva et al., 2011). The existence of sharp Braggs peak indicates that epoxy still retain an intercalated structure after mixing with CB. But some the secondary diffraction peak is weakened or even disappears with increase of CB concentration. Secondary diffraction peak is contributed to crystallization to the system. Hence, the present of epoxy filler will alter the structure in epoxy system as well as the crystanallity of epoxy.

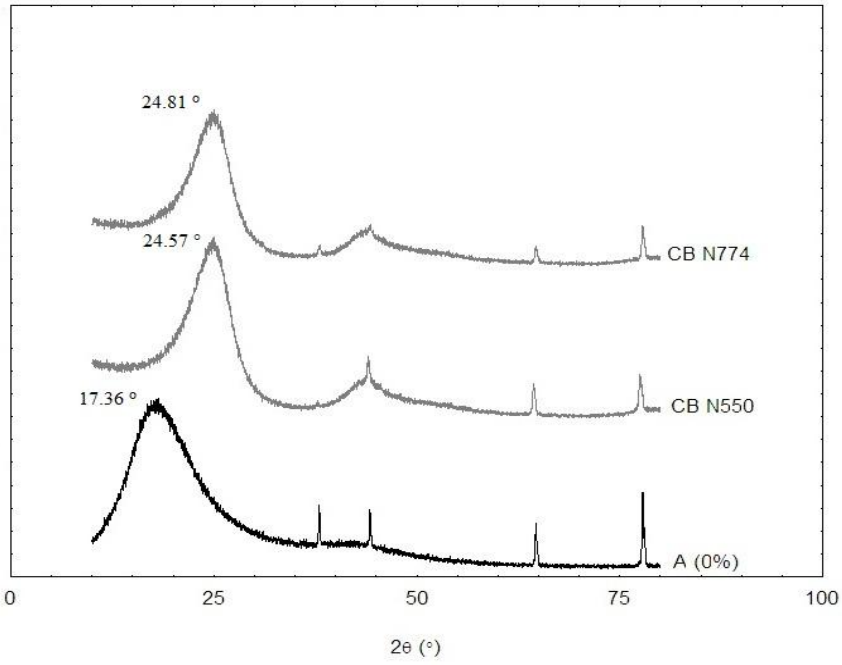

Figure 4.16: XRD Patterns for CB fillers and Neat Epoxy

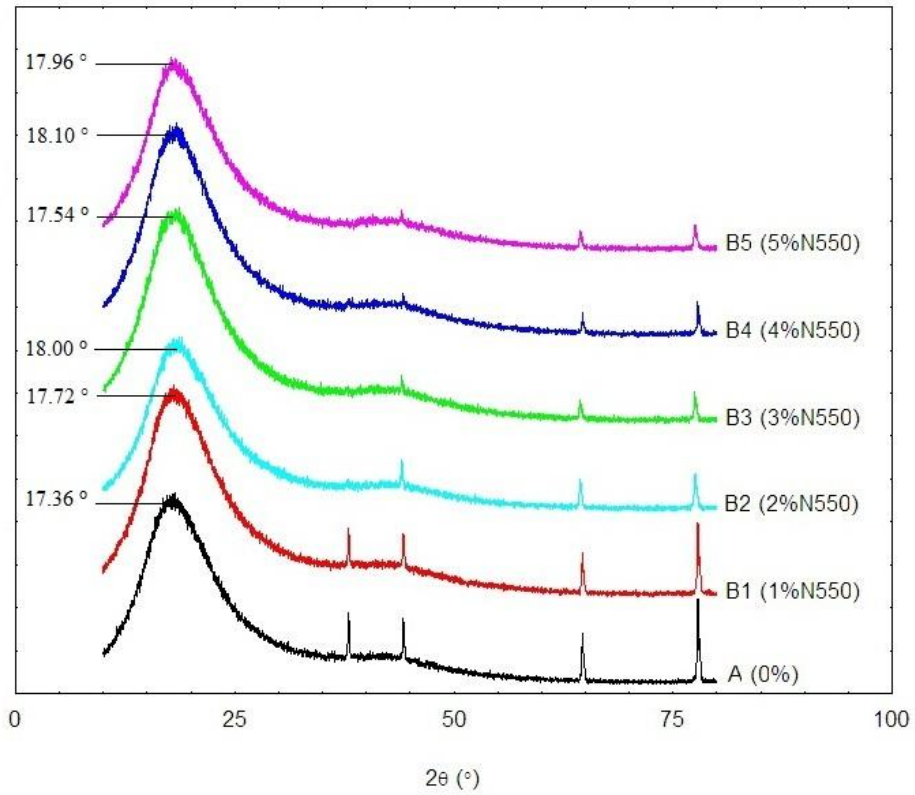

Figure 4.17: XRD Patterns for CB N550-Epoxy Composites

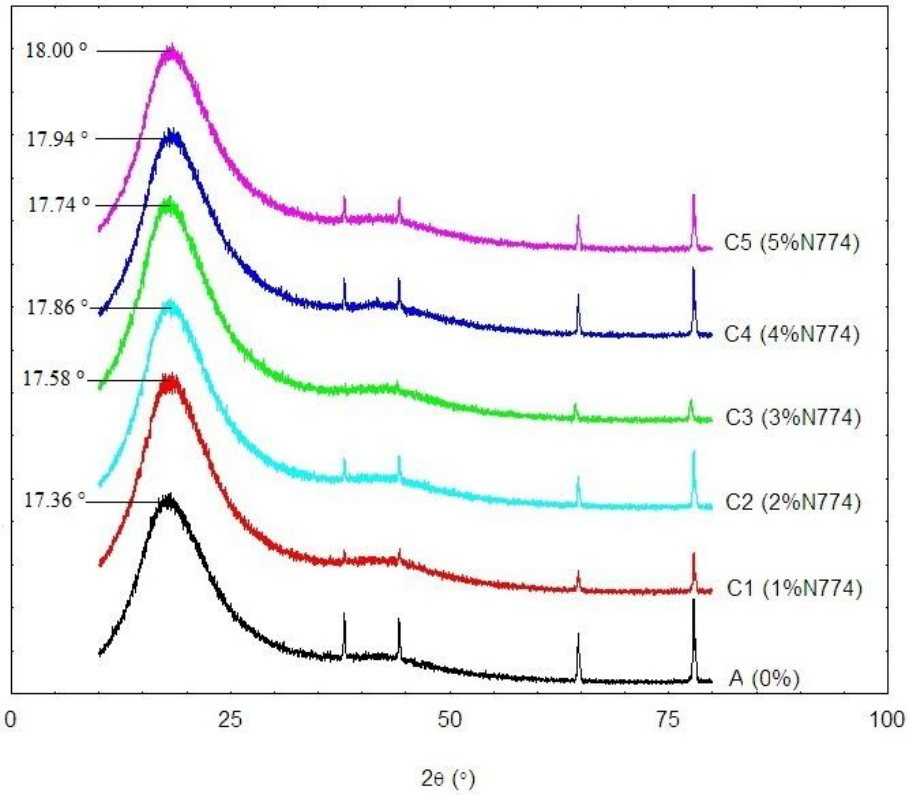

Figure 4.18: XRD Patterns for CB N774-Epoxy Composites

Table 4.1: XRD Pattern Peak (°) of Carbon Black-Epoxy Samples

Sample	Formulation	Peak (°)
A	0 wt.%	17.36
CB N550	100 wt.% N550	24.57
B1	1 wt. % N550	17.72
B2	2 wt. % N550	18.00
B3	3 wt. % N550	17.54
B4	4 wt. % N550	18.10
B5	5 wt. % N550	17.96
CB N774	100 wt.% N774	24.81
C1	1 wt. % N774	17.58
C2	2 wt. % N774	17.86
C3	3 wt. % N774	17.74
C4	4 wt. % N774	17.94
C5	5 wt. % N774	18.00

4.2.2 Effect of Carbon Black on Crystallization

From Figure 4.7 and 4.8, the secondary diffraction peak was decreased with the additional of CB filler. The crystallinity is related with the secondary diffraction peak. This indicates that the property of epoxy is being swift to amorphous behaviour. The overall crystallinity of CB N550-epoxy composites is lower than CB N774-epoxy composites. From Table 4.2 we can study that, the crystallinity of neat epoxy is highest among all formulation which indicates the structure of neat epoxy is in a well arrangement. With the mixing with CB, the forming of well organize matrix structure during curing process is being interrupt. crystallinity percentage of CB N550-epoxy composite was decreased with the increasing of CB concentration. However, for CB N774 composites, the crystallinity was decreased in an unorganised trend. From the SEM study, it can be realised that the larger size compare to CB N550 decrease the dispersion rate hence can results better curing degree for the curing process of epoxy. Besides that, the random distributions of large particle also contribute in the random crystallinity of CB N774-epoxy composite but the overall crystallinity was

decreasing with addition filler. The CB N-550 able to lower down crystallinity of epoxy with a trend due to its high dispersion rate and small particle size.

Table 4.2: Crystallinity (%) of Carbon Black-Epoxy Samples

Sample	Formulation	Crystallinity (%)
A	0 wt.%	7.21
CB N550	100 wt.% N550	6.91
B1	1 wt. % N550	6.51
B2	2 wt. % N550	6.31
B3	3 wt. % N550	5.46
B4	4 wt. % N550	5.52
B5	5 wt. % N550	5.12
CB N774	100 wt.% N774	6.50
C1	1 wt. % N774	5.88
C2	2 wt. % N774	6.15
C3	3 wt. % N774	5.50
C4	4 wt. % N774	6.20
C5	5 wt. % N774	5.97

4.3 Rheology

4.3.1 Viscosity of Carbon Black-Epoxy Composite

4.3.1.1 Effect of Carbon Black Concentration on Viscosity

The filler concentration has a great effect on viscosity and other mechanical properties of polymer. The filler increase the viscosity with the increasing of volume occupied by the filler (Bullard et al., 2009). In this study the weight percent (wt.%) of CB was manipulated to find out its effect on viscosity of epoxy. As the weight percent of filler was increase and being stirred vigorously the volume occupied by

the filler in epoxy was increased as well. The CB N550 and N774 which mixed with epoxy in this study proved the theory significantly as shown in Figure 4.19 and 4.20.

The viscosity of epoxy increased with increasing of filler concentration. With the filler concentration increase from 1 wt.% to 5 wt.%, the viscosity was increasing follow the trend. As can be seen, for the initial reading of viscosity, both of the filler (N550 & N774) with 5 wt.% gave the highest reading of viscosity. With increasing concentration of filler, the inter-particle interaction was increased. This behaviour has been observed for other carbon based nanoparticles dispersed in epoxy resins, including spherical particles and carbon nanotubes (Abdalla et al., 2007; Song & Youn, 2005; Kim, Seong, Kang, & Youn, 2006; Kotsilkova, Fragiadakis, & Pissis, 2005). The Inter-particle interaction force is much more depends on the surface area and collision of fillers. Collision of CB happens rapidly with increasing of the CB concentration. When collide, CB tends to form aggregates which provide strong linkage to epoxy system and lead to increase of the viscosity. The matrix structure of CB contributes to high viscosity reading in the test. This statement also supported by SEM study in previous section.

From Figure 4.19, viscosity of neat epoxy is higher than 1 wt.% of N550. The viscosity of neat epoxy and 1 wt.% N550 is extremely low which are 0.842 and 0.781 Pa.s.; Due to the viscosity of CB-epoxy composites is extremely sensitive to curing time a few second different of experiment time can lead to overtake of neat epoxy values. Hence, the differences of viscosity at initial values might not be obvious and adequate.

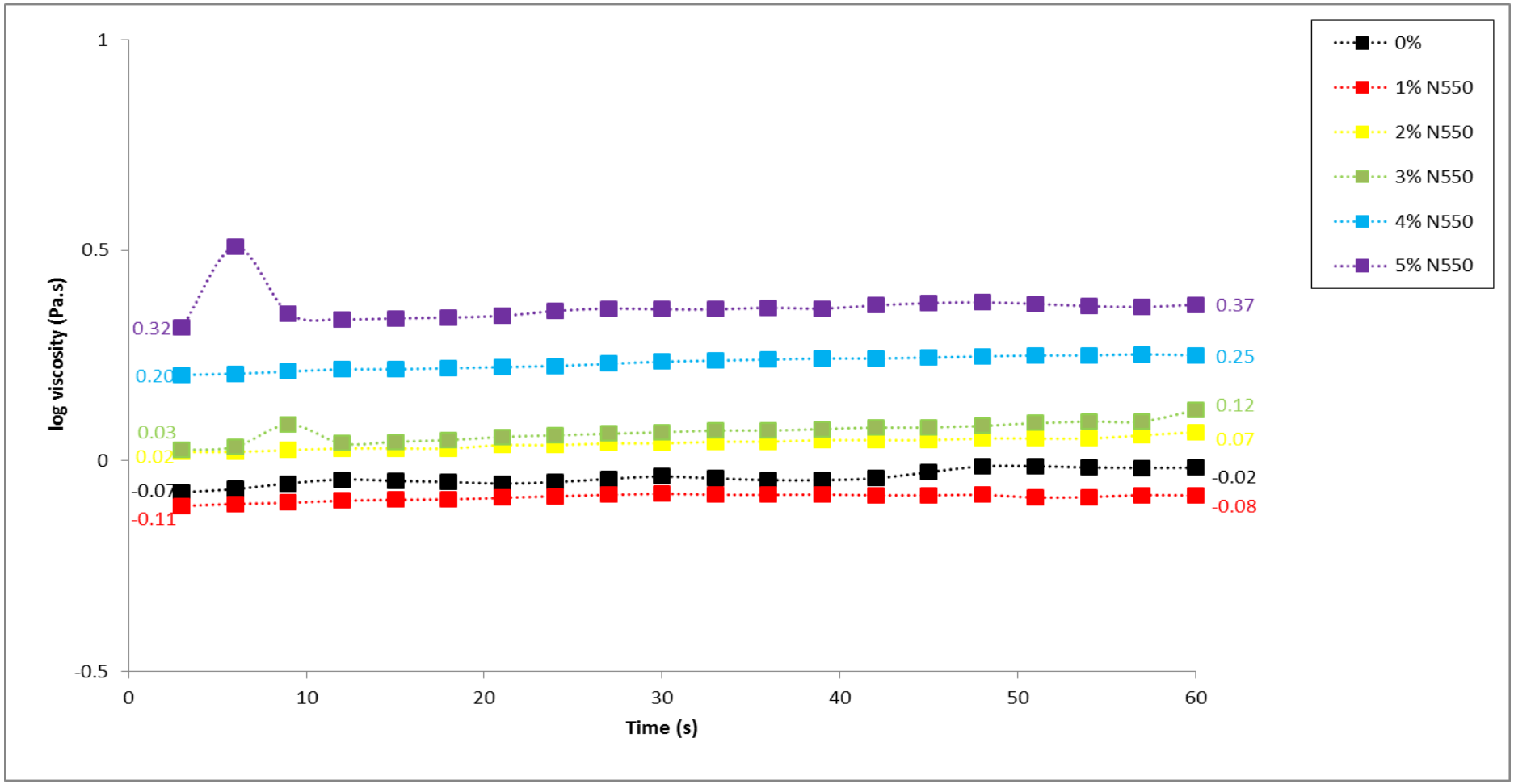

Figure 4.19: Initial Viscosity of CB N550-Epoxy Composites

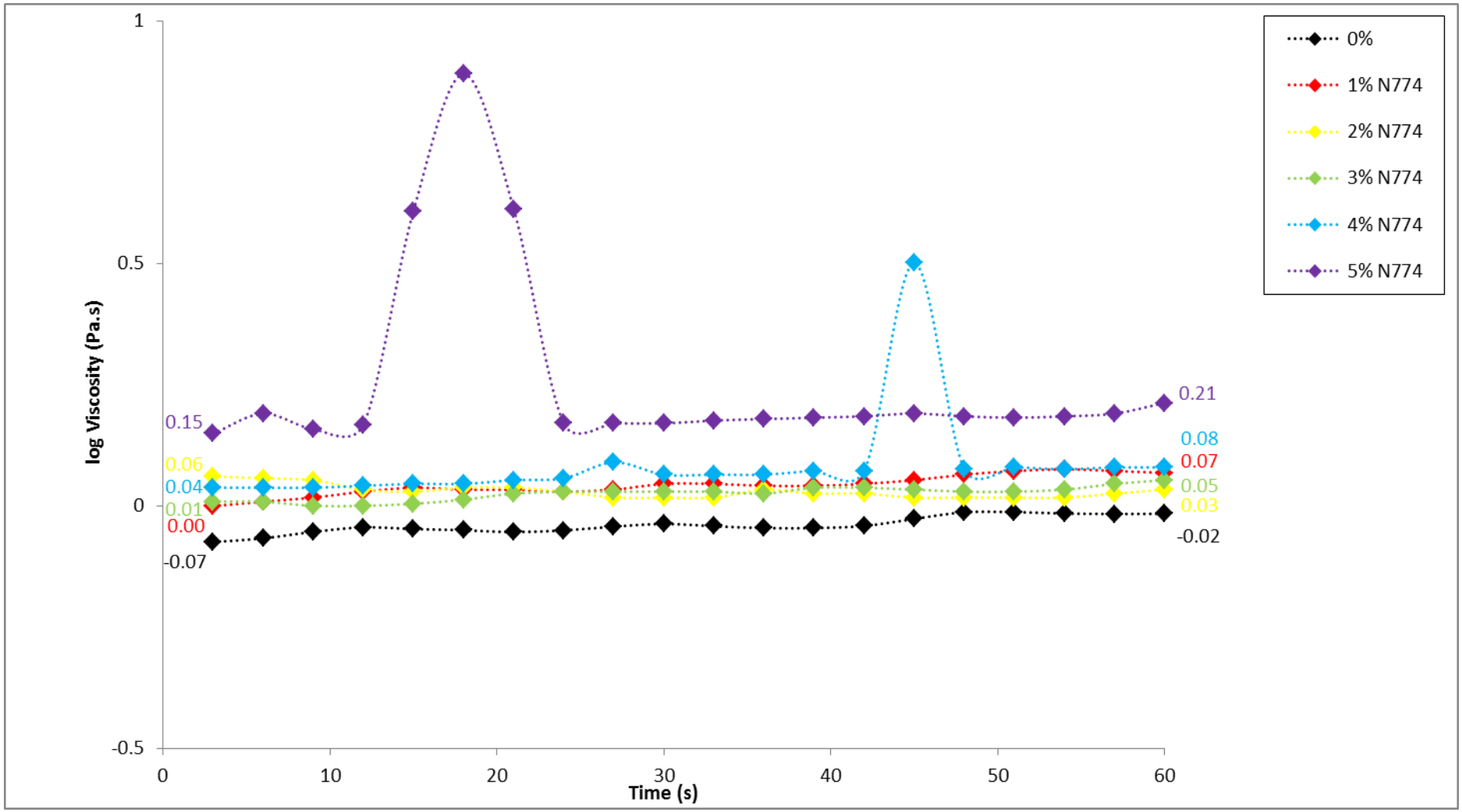

Figure 4.20: Initial Viscosity of CB N774-Epoxy Composites

4.3.1.2 Effect of Carbon Black Particle Size on Viscosity

Two CB used in the study which are N550 and N774 have different particle size. The smaller filler particles have larger surface area. It increases the contact between particle in polymer and form bond more easily (Durairaj et al., 2010). With more interaction between particles, viscosity of epoxy with smaller filler particles will be higher than that with larger filler particles. CB N550 and N774 have an average molecular size of 53 nm and 110nm.

By comparison of initial viscosity curve as shown in Figure 4.21, 5 wt.% N550-epoxy composites indicate higher viscosity reading compare to 5 wt.% CB N774-epoxy composites at the same concentration. The smaller particle size allows the filler disperse better in epoxy system and have larger surface area. Large surface area provide a higher chances of aggregation and form matrix structure which lead to high viscosity of the epoxy system. Higher surface area of filler can form stronger attraction force to epoxy results in resistance of flow and high viscosity. On the other hand, larger particles have smaller surface area which is hard to aggregate and form weaker forces to epoxy. So, larger filler (CB N774) has lower viscosity compare to smaller filler (CB N550).

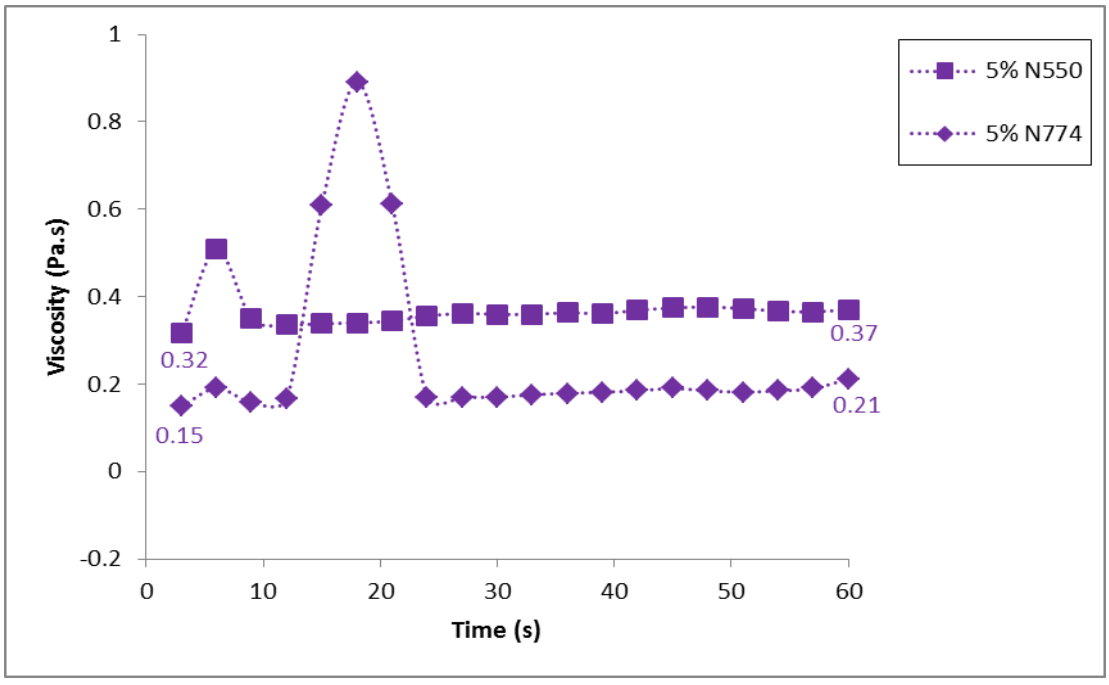

Figure 4.21: Comparison of Initial Viscosity at 5 wt.% CB-Epoxy Composites

Besides that, the rate of viscosity increment by increasing concentration CB N774 is less than CB N550. This can be observed in Figure 4.19 and 4.20. The flow curve gap between different CB N774 concentrations is smaller than the flow curve gap of CB N550. From the study, as the particle size of filler decrease, the viscosity increase under same concentration but the statement does not fully apply after curing of CB-epoxy composite.

4.3.1.3 Effect of Cross Linking Agent on Viscosity

The viscosity readings were taken for 2 periods which is initial reading and after 1 hour curing time of CB-epoxy composite. For initial reading, the viscosity increase with the increasing of CB concentration. At the time, effect of cross linking agent is still not visible due to chemical reaction between epoxy resin and curing agent were not yet take place. Chemical reaction with the present of cross linking agent increase the viscosity of epoxy and shifted it phase from liquid to liquid-gel composite and stable at solid form after fully cured. The effect of cross linking agent on CB N550/N774-epoxy composites can be found out from Figure 4.22 and 4.23.

At the intermediate of 60 second testing period, small peak of viscosity might be obtained. The peak reading in flow curve is due to incomplete curing process in epoxy. The epoxy is partially cured or have a small amount of cured epoxy particles formed that provide a great resistance force to the flow results in peak of flow curve. Those peaks reduce back to its original position after few second of the test. Those small amounts of highly cured epoxy particles are being break down into smaller particle as other epoxy particles and disperse evenly within the sample because it could not resist the forces apply on it.

After 1 hour of curing, those samples undergo viscosity test to study the effect of curing agent on epoxy. Viscosity was increased dramatically for all of the samples. It proved that the chemical bonding between curing agent and epoxy were increased during the 1 hour period (Dijkhuis, Noordermeer, & Dierkes, 2009).

Although uniform peaks in flow curve were still exist due to highly cured epoxy particles compare to other particles, the flow curve was rather consistence compare to flow curve at initial reading because the solid-like cured epoxy produced during curing period is distribute evenly in the samples and contribute to increase of viscosity like filler. Large amount of flocculated cured particles provide higher resistance forces to the flow and gave higher viscosity reading.

Unlike the initial reading of viscosity, readings after 1 hour do not completely obey the rule of higher concentration of filler brings to higher viscosity value. Viscosity of neat epoxy is not the lowest compare to both CB-epoxy composites. For CB N550 series, viscosity of neat epoxy is only slightly lower than 5 wt.%. For CB N774 series, flow curve of 1 wt.% and 2 wt.% are position at below neat epoxy. The high viscosity of neat epoxy after 1 hour curing was due to absent of foreign particles that decrease the rate of flocculation forming during curing period. Foreign particles like CB can block the aggregation of partially cured epoxy and results in slow down of curing process. Smaller size of filler disperses better in epoxy system and increase viscosity by increasing concentration at initial reading. The high dispersing rate of small size filler bring negative impact to viscosity of epoxy at curing period. Viscosity of CB N774 series is higher than CB N550 series. Large particles of filler allow curing agent function more effectively. Hence shorter time required to reach higher curing degree of the CB-epoxy composite. Neat epoxy can reach same curing degree in the shortest time.

However, neat epoxy did not have highest viscosity after 1 hour of curing time among all samples even the filler brings side effect to viscosity of epoxy or to be in precise, filler increase the curing time needed to reach the same curing degree compare to neat epoxy. High concentration of filler still gave the highest viscosity at 1 hour after curing. Positive effect of increase concentration at 5 wt.% and above of CB N550 as well as 3 wt.% and above of CB N774 is much more greater than its side effect. The resistance of flocculate formation was much lower than the positive effect of increase filler concentration. It results in the viscosity of neat epoxy was higher than certain concentration of filler but not all concentration.

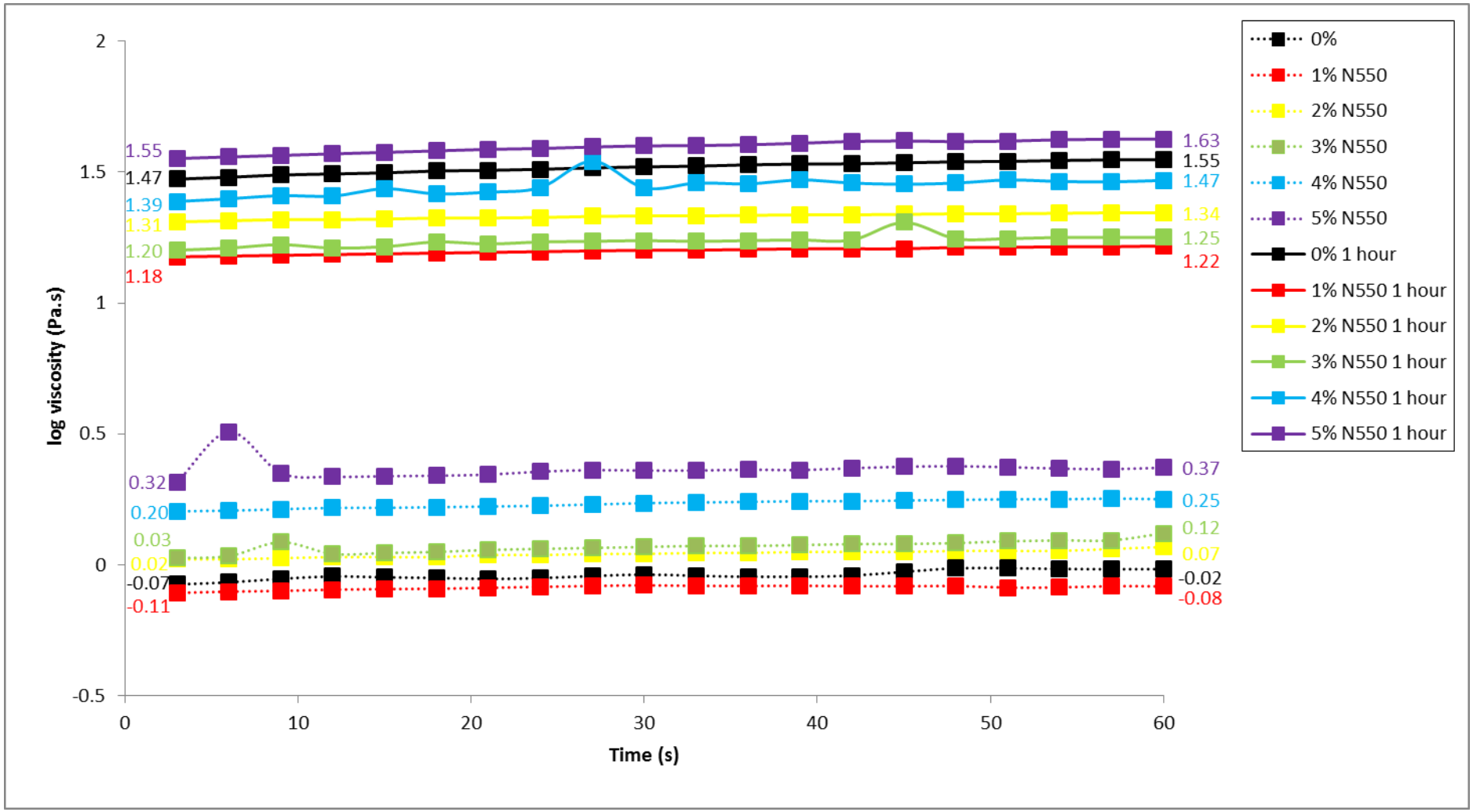

Figure 4.22: Comparison of Initial Viscosity of CB N550-Epoxy Composites and Viscosity after 1 hour of Curing

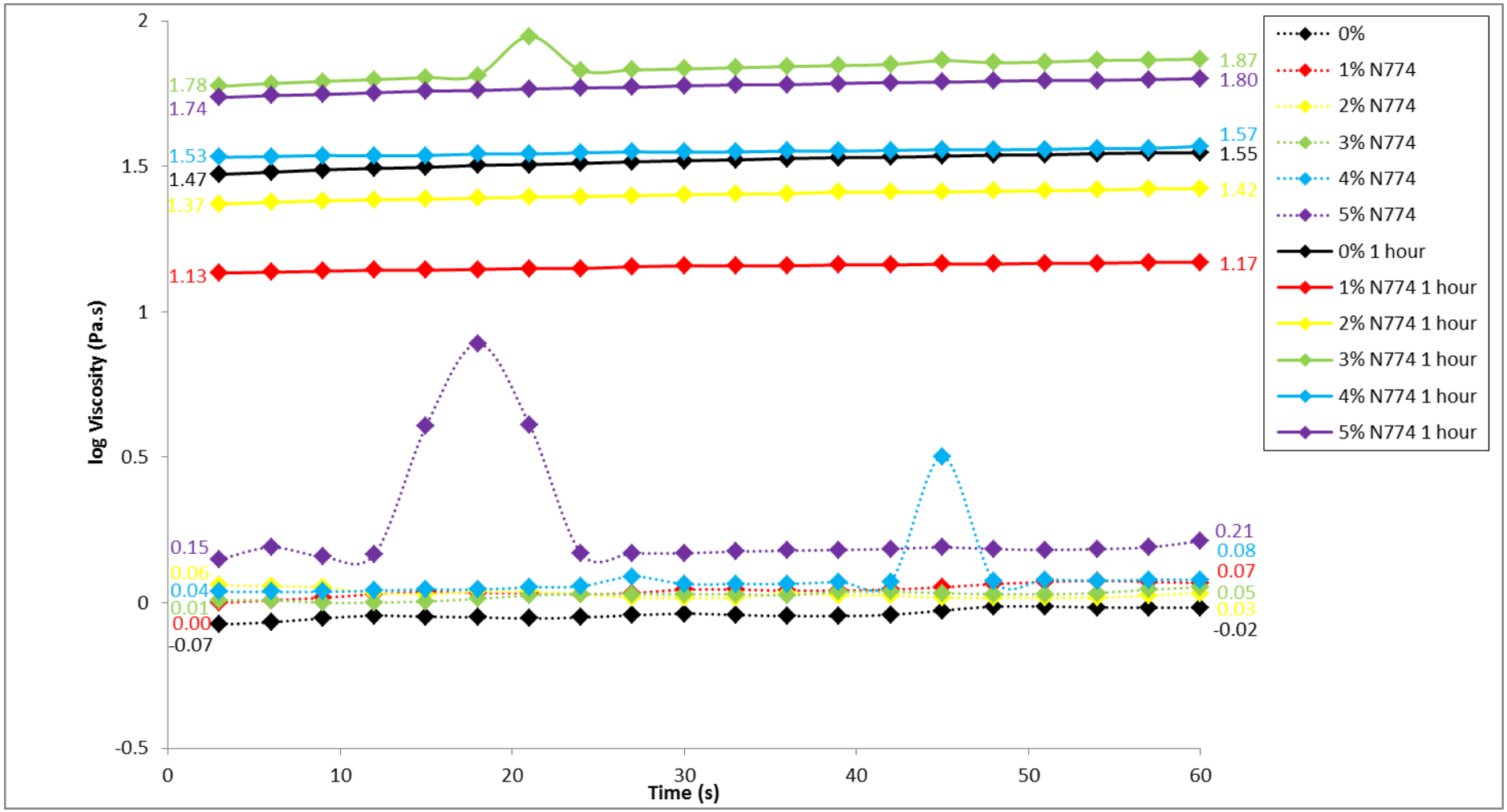

Figure 4.23: Comparison of Initial Viscosity of CB N774-Epoxy Composites and Viscosity after 1 hour of Curing

4.3.2 Viscoelastic Behaviour of Carbon Black-Epoxy Composite

4.3.2.1 Effect of Carbon Black on Viscoelastic Behaviour

Phase angle is use to indicate the elastic behaviour of a material with higher degree show more viscos-like properties. CB-epoxy composites show viscoelastic behaviour in all formulation by phase angle lies in between 0 ° to 90 ° which are shown in Figure 4.24, 4.25, 4.26 and 4.27. Both of 5 wt.% filler indicate the lowest reading of phase angle at initial which indicates the high concentration of filler prevent the solid-like epoxy to shift into viscos-like behaviour. The differences of phase angle for all concentration are significant at initial reading.

At low shear strain, the storage moduli of CB N550 and N774-epoxy composites are higher than the loss moduli which show elastic behaviour of the polymer. With the increasing of shear strain, storage modulus gave lower value than loss modulus. Figure 4.28 and 4.29 show CB-epoxy composite behaviour which is pseudo solid-like (G'>G") under low strain but with increasing of shear strain, the rheological behaviour was changed to a pseudo liquid-like behaviour (G">G') (Franchini et al., 2009). This kind of flow character is categorised as thixotropy properties because the applying of forces is able to break the attraction force between epoxy and CB. This character is shown by all formulation of CB-epoxy composites. At a high shear rate, no pseudo solid-like behaviour was observed because the matrix structures in CB-epoxy were completely ruptured. Consequently, the CB-epoxy composite overturn into a liquid behaviour.

With increasing the concentration of filler into epoxy system, it is not only change the viscosity but also lead to deviation from Newtonian behaviour such as shear-thinning or shear-thickening behaviour (Kotsilkova et al., 2005). From studies, loss modulus, G' and storage modulus, G" increase with increasing of filler or additive (Shahzada, Bohidar, & Agnihotry, 2006). From Figure 4.28 and 4.29, initial modulus of 5 wt.% of filler for both CB N550 and N774 gave the highest value among other formulation and neat epoxy. The CB-epoxy composites became more viscous (higher G" values) and more elastic (higher G' values) with the present of

filler. CB particles added into the epoxy system percolate in a three-dimensional network cause to the appearance of pseudo solid-like behaviour (Franchini et al., 2009).

For storage modulus (G') and loss modulus (G"), after the shear strain increase, it enters a random value gap before it stable due to uneven distribution of cured epoxy particles. Both of the curves enter a stable trend after certain strain percentage was applied on it. Loss modulus (G") means the ability of the material to dissipate energy. The G" values were increasing until a limit and remain constant with increasing of shear strain. It implies that the ability to release energy of CB-epoxy composites is increase with the increasing of shear strain. Storage modulus (G') is the measure of elasticity material. The G' value is inversely proportional with shear strain. While the G" is increasing with shear strain, G' was decreasing until G" was overtaken its value.

Apart from that, by increasing the concentration of CB, the solid-like behaviour is enhanced. The CB particles formed more aggregates by increase CB concentration. The inter-particle force of CB is not only enhancing the strength of itself but also strength up the interface adhesion with epoxy. Although the enhancement are not strong enough to maintain the matrix structure of epoxy with increasing of shear strain, the G' values were increased with increasing of filler concentration. The G" value was low at the initial; it is because the viscous behaviour of epoxy system is not obvious. After adding on stress on the paste, CB particles in the system breaking down from its matrix structure and acted as a lubricant in CB-epoxy system. Hence the viscosity and the elastic properties can both increase with the increasing of CB concentration.

However, type of filler does not affect much to the modulus except for CB N550-epoxy composites show a slightly higher value than CB N774-epoxy composites. The manipulating factors are size of filler and surface area of filler. Smaller size of filler tends to disperse better in epoxy system hence results in stronger elastic behaviour. The large surface area allows the CB particles easier to stack and aggregate hence the elastic behaviour was increased.

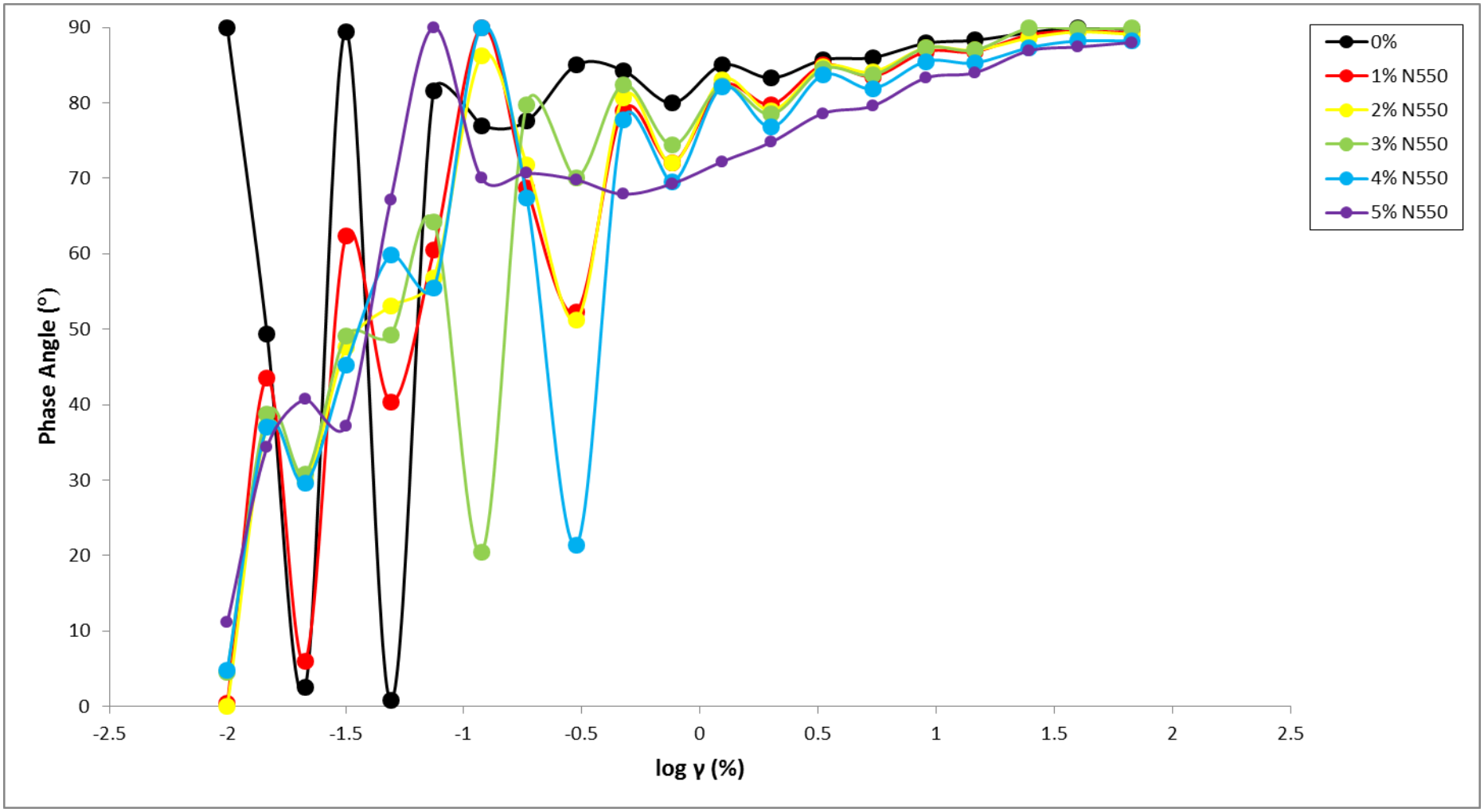

Figure 4.24: Initial Phase Angle ( ) of CB N550-Epoxy Composites

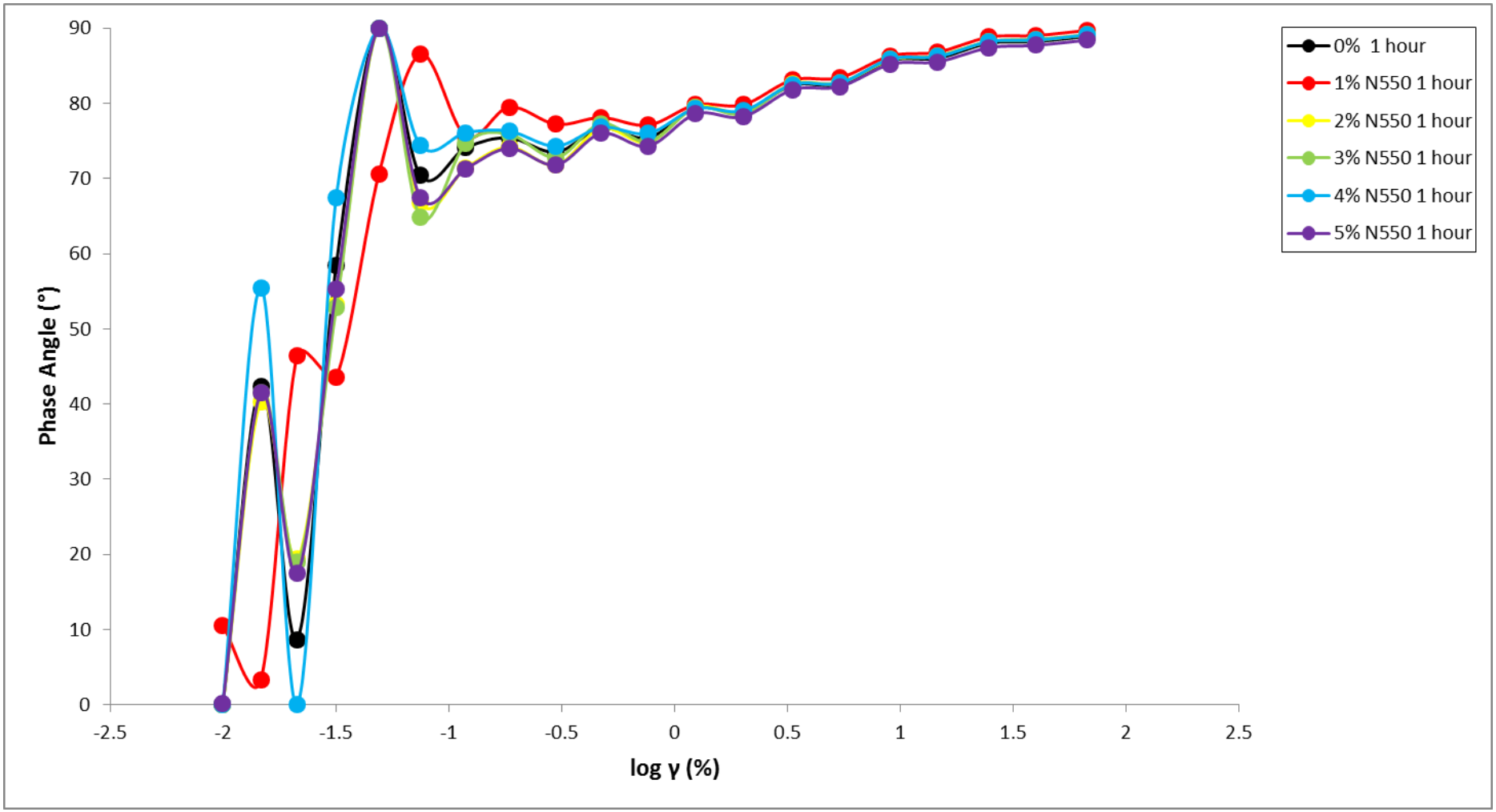

Figure 4.25: Phase Angle ( ) of CB N550-Epoxy Composites after 1 Hour of Curing

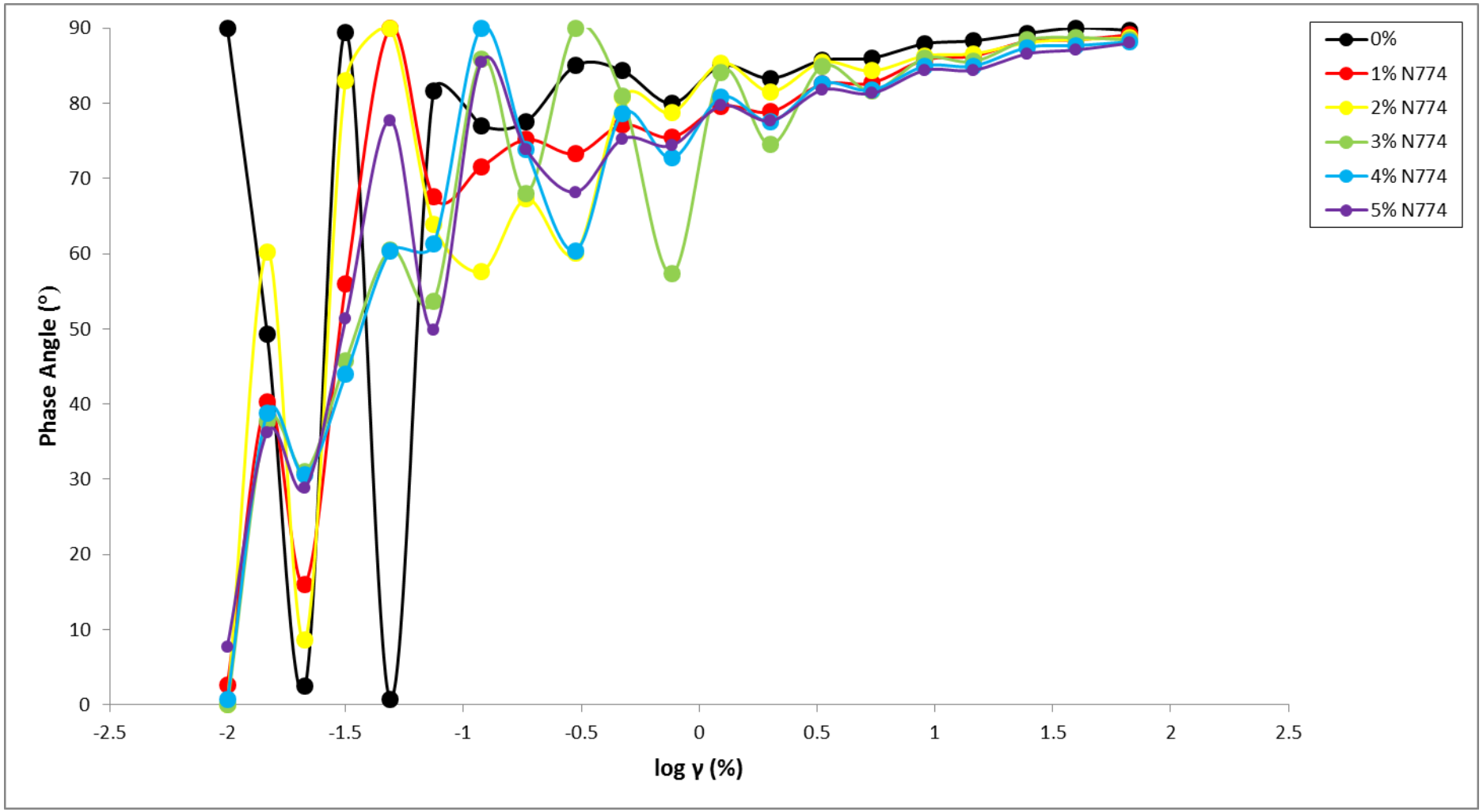

Figure 4.26: Initial Phase Angle ( ) of CB N774-Epoxy Composites

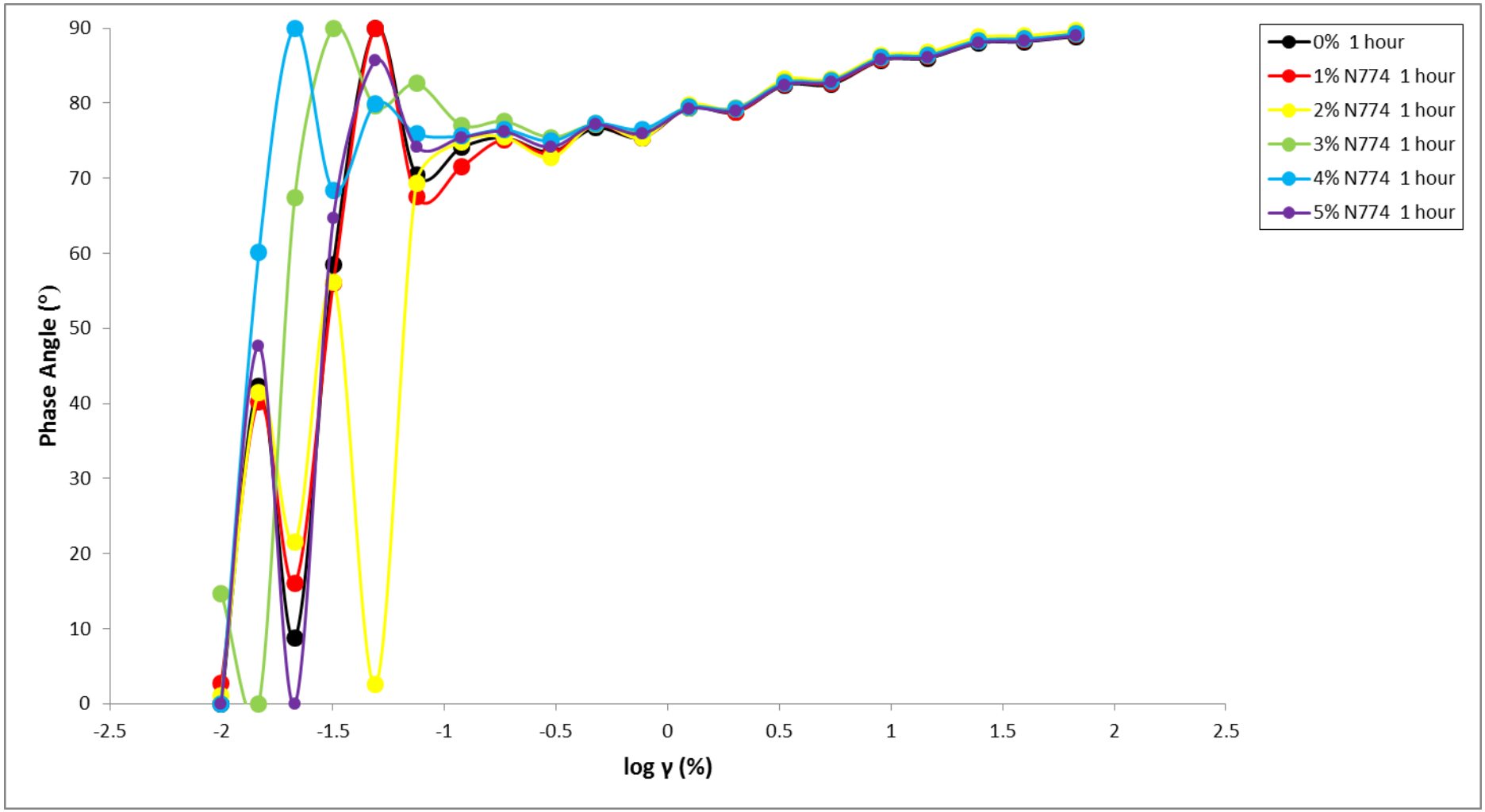

Figure 4.27: Phase Angle (ᵟ) of CB N774-Epoxy Composites after 1 Hour of Curing

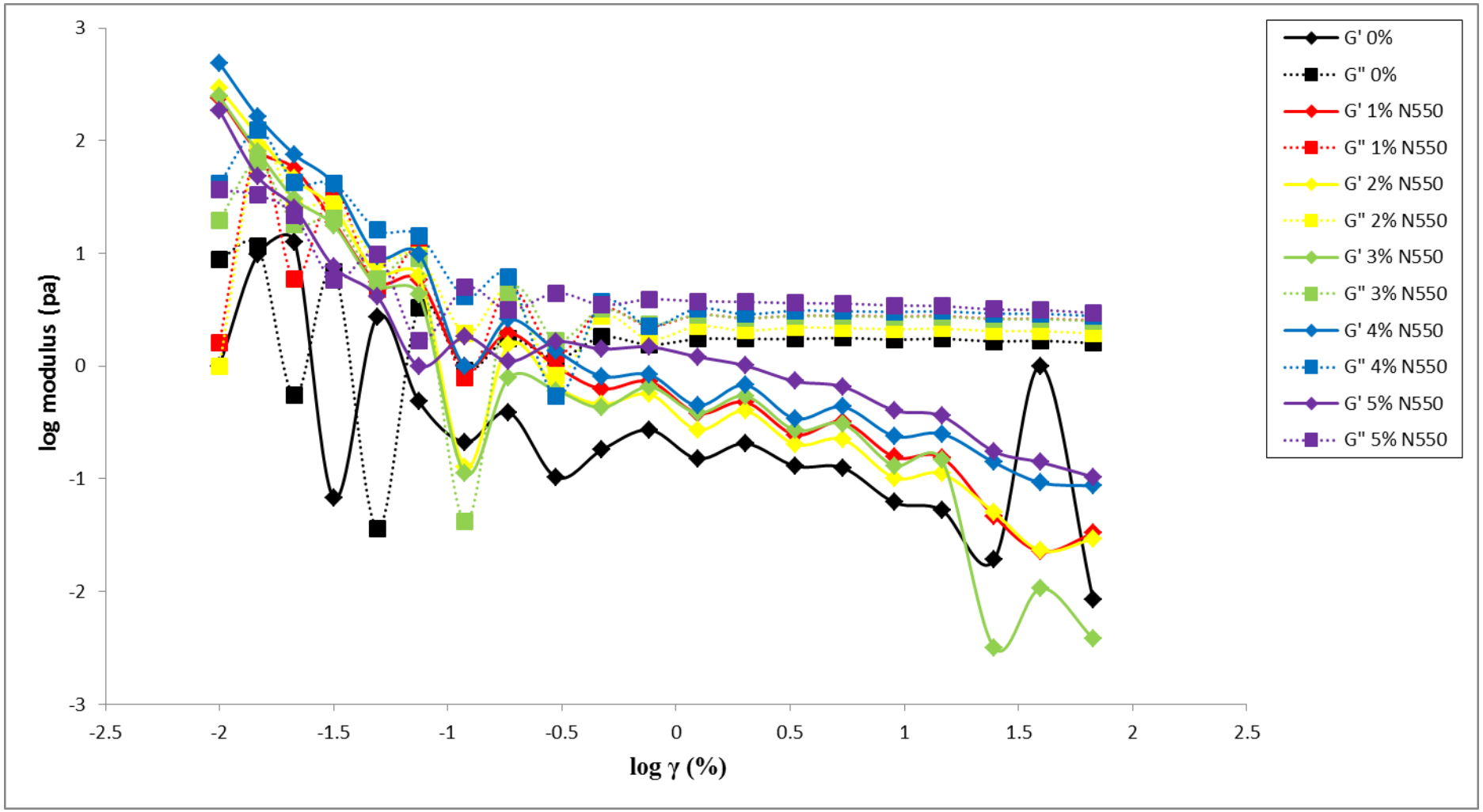

Figure 4.28: Initial Modulus of CB N550-Epoxy Composites

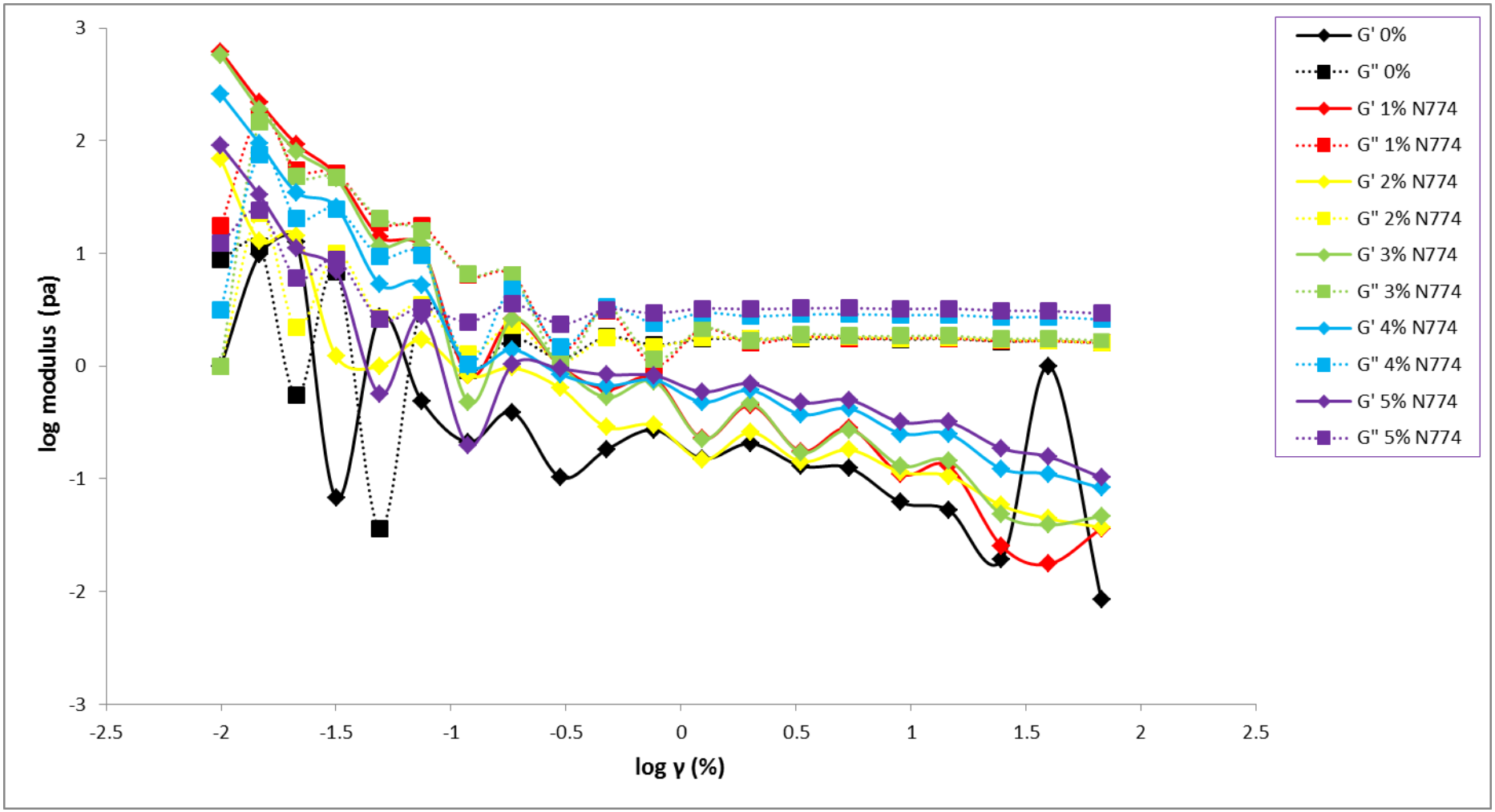

Figure 4.29: Initial Modulus of CB N774-Epoxy Composites

4.3.2.2 Effect of Cross Linking Agent on Viscosity

Similar to viscosity, viscoelastic behaviour are strongly affected by cross linking. The effect of CB on viscoelastic behaviour became less significantly which shows at Figure 4.27 and 4.29. After the strain increased, the difference of phase angle at various concentrations showed in initial reading was decreased. All formula shows the similar phase angle after 1 hour of curing. The decrease of filler effect is results by flocculation of solid-like epoxy act like filler and occupied the epoxy system.

The introducing of cross linking agent into epoxy resin is not only change the viscosity but also lead to deviation from Newtonian behaviour such as shear thinning. From Figure 4.30 and 4.31, we can notice the changing of G' and G" curve after 1 hour of curing is different with its initial trend. The G' and G" values for all formulation after 1 hour of curing enter the stable condition at lower shear strain percent compare to initial modulus. Besides that, the values of G' and G" also increase significantly after curing for 1 hour. The chemical reaction between epoxy and curing agent in the system during curing process plays a great role in this phenomenon.

At the other hand, the G' curve have a greater change after 1 hour of curing. Overall value of G' increased in all CB compositions including of neat epoxy. Unlike the initial values of G', G' after 1 hour of curing did not decrease all the way but remain constant for a period of time before the elastic property degraded as shown in Figure 4.32. The resistance force of epoxy towards degradation is higher compare to initial reading. During the 1 hour curing time, high degree of curing and flocculated cured particles distribute more uniformly cause the epoxy stay in elastic behaviour before it being degraded by the shear strain.

As mention above, particle size of filler will affect the viscosity of CB-epoxy composites. Without any doubt, viscoelastic behaviour is affected by curing agent as well. Both the modulus of neat epoxy is only slightly lower than 5wt.% of CB N550. Modulus of 1wt.% and 2wt.% are position at below neat epoxy, for CB N774 series which we can notice from Figure 4.30 and 4.31. The curing process was slowed down by CB particles. With the increasing of particle size, the speed down is less

significant to the curing process. The side effect of CB will be overcome by high concentration of filler. In general, below stress limit of the epoxy system it behaves as a solid, but at high shear rates a liquid-like behaviour takes place (Chapartegui et al., 2010).

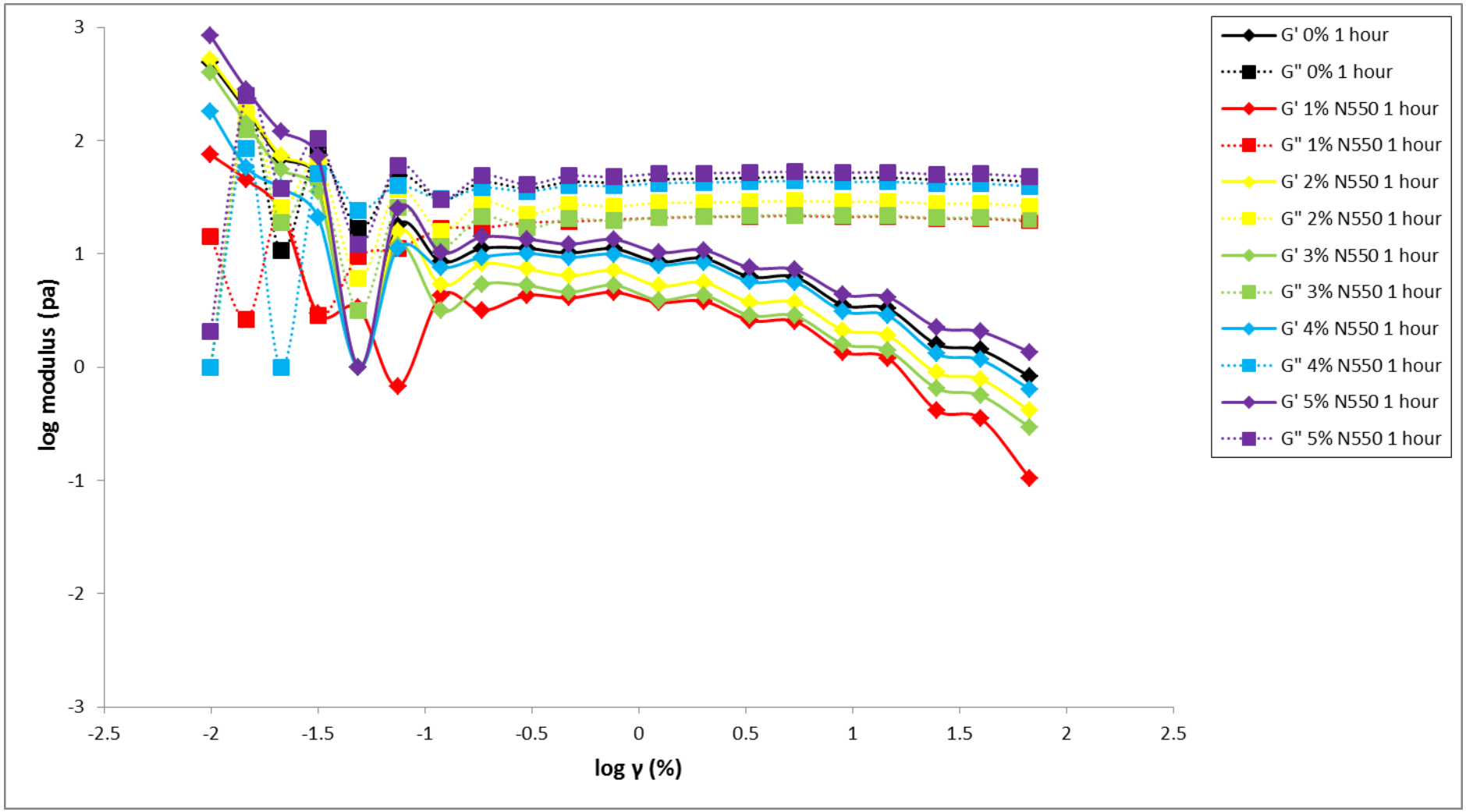

Figure 4.30: Modulus of CB N550-Epoxy Composites after 1 Hour of Curing

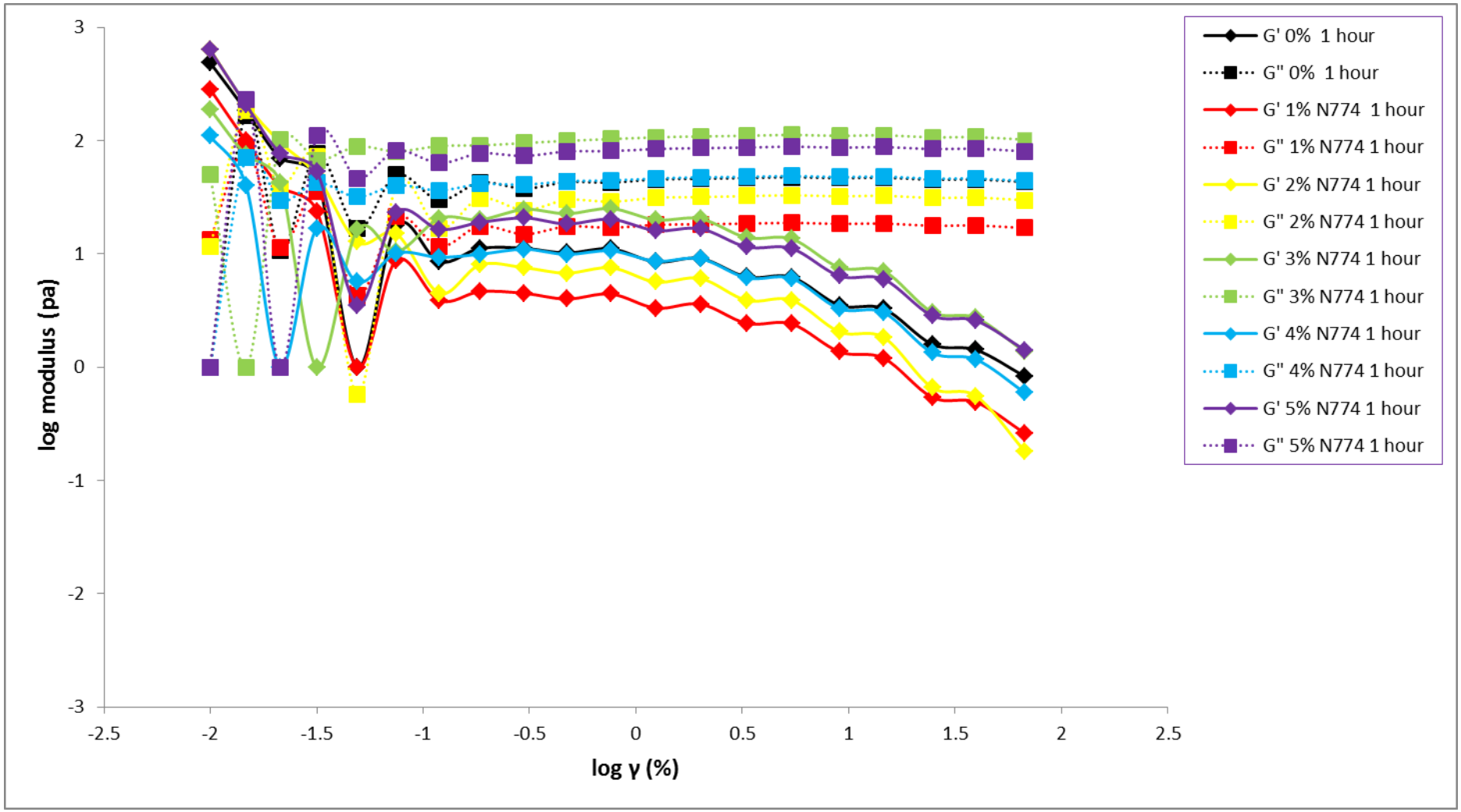

Figure 4.31: Modulus of CB N774-Epoxy Composites after 1 Hour of Curing

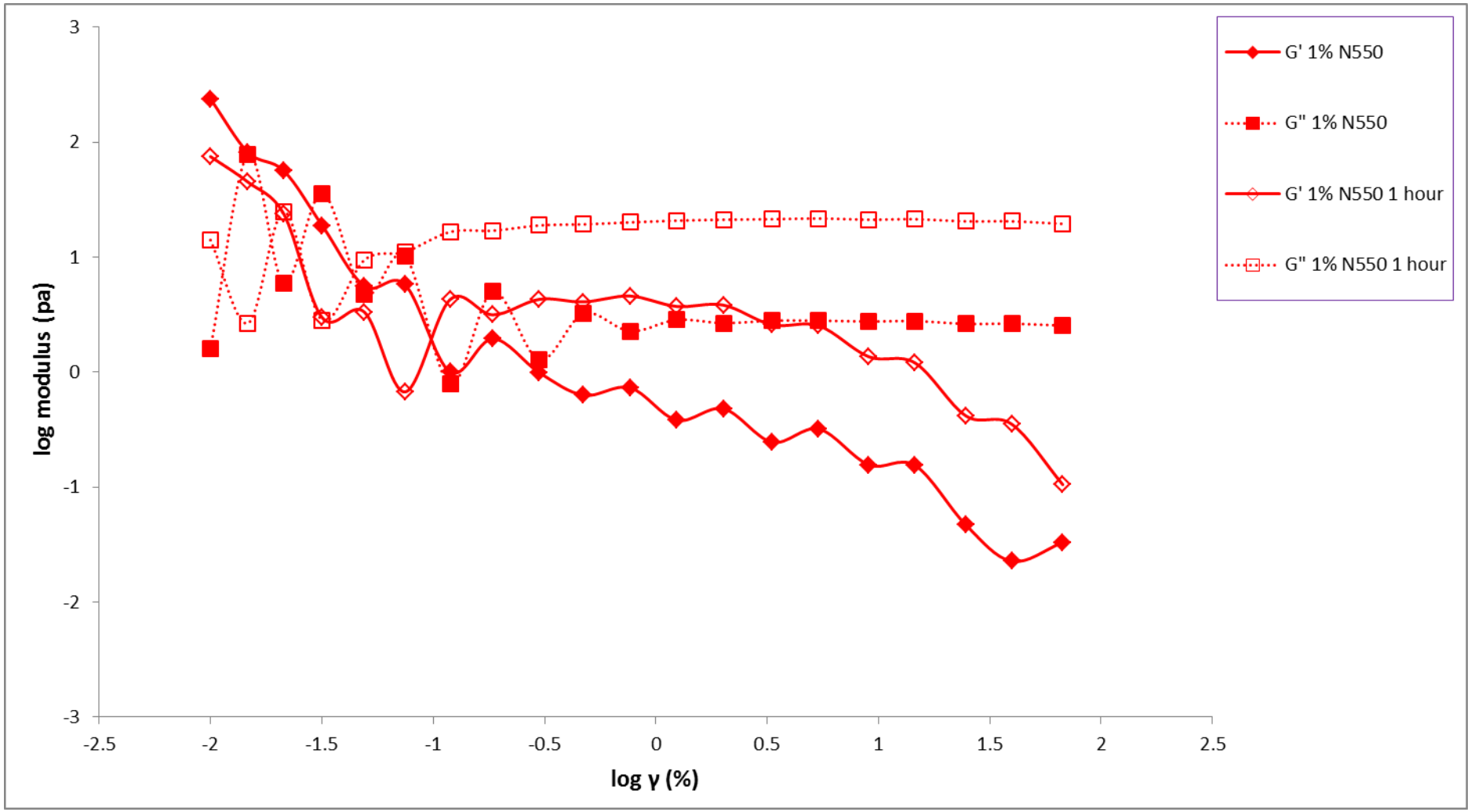

Figure 4.32: Modulus Comparison of 1 wt.% CB N550-Epoxy Composites at Initial and after 1 hour of Curing

CHAPTER 5

CONCLUSION AND RECOMMENDATIONS

5.1 Conclusion

Several conclusions can be made from results of the current research presented in thesis:

1) Smaller particle size of filler tends to disperse better in epoxy system.
2) Fillers will decrease the crystallinity of epoxy system.
3) Rheological properties such as viscosity, G' and G" were in higher values by increasing of filler (CB).
4) Epoxy added with smaller size filler (CB N550) has higher viscosity, G' and G" at initial time but epoxy mix with larger filler (CB N774) obtained higher viscosity, G' and G" after 1 hour of curing.
5) Rheological properties (viscosity and modulus) were in higher values by cross linking process.

5.2 Recommendations

Some of the test could not be done in this study due to time and budget constraint. In future studies, the mechanical properties testing like tensile test and thermogravimetric analysis (TGA) should be done to identify changes of the mechanical strength and thermal properties of the CB-epoxy composites. Thus, the

maximum amount of CB can be added into the epoxy without scarifying the desire mechanical properties would be identified.

In addition, rheological test of the epoxy should be done in aging in order to investigate the changing of rheological properties regards to the time due to curing process is extremely sensitive to time. For CB, Brunauer, Emmett and Teller (BET) method can be used to determine the average particles surface area of filler to further characterize the results. Besides, electrical properties should be studies for the samples (epoxy) which always uses as coating materials, insulator and printed circuit.

REFERENCES

Abdalla, M., Dean, D., Adibempe, D., Nyairo, E., Robinson, P., & Thompson, G. (2007). The effect of interfacial chemistry on molecular mobility and morphology of multiwalled carbon nanotubes epoxy nanocomposite. *Polymer, 48,* 5662-5670.

Abdul Khalil, H., Firoozian, P., Bakare, I., Md. Akil, H., & Md. Noor, A. (2010). Exploring biomass based carbon black as filler in epoxy composites: Flexural and thermal properties. *Materials and Design, 31,* 3419-3425.

ASTM International . (2005a). *Standard Calssification System for Carbin Blacks Used in Rubber Products.* Philadelphia, PA: American Society for Testing and Materials.

Auchter, J. (2005). *Chemical Economics Handbook: Carbon Black.* Menlo Park, CA: SRI Consulting.

Bao, X., Lee, N., Raj, R., Rangen, K., & Maria, A. (1998). Engineering solder paste performance through controlled stress rheology analysis. *Journal of Solder Surface Mount Technology, 10,* 26-35.

Bullard, J., Pauli, A., Garboczi, E., & Martys, N. (2009). Comparison of viscosity-concentration relationships for emulsions. *Journal of Colloid and Interface Science, 330,* 186-193.

Chapartegui, M., Markaide, N., Florez, S., Elizetxea, C., Fernandez, M., & Santamar á, A. (2010). Specific rheological and electrical features of carbon nanotube dispersions in an epoxy matrix. *Composites Science and Technology, 70,* 879-884.

Dannenberg, E. (1978). *Kirk-Othmer Encyclopedia of Chemical Technology* (3rd ed., Vol. 4). New York: John Wiley & Sons.

Dijkhuis, K. A., Noordermeer, J. W., & Dierkes, W. K. (2009). The relationship between crosslink system, network structure and material properties of carbon black reinforced EPDM. *European Polymer Journal, 45*, 3302-3312.

Durairaj, R., Lam, W., Ekere, N., & Malik, S. (2010). The effect of wall-slip formation on the rheological behaviour of lead-free solder pastes. *Journal of Materials and Design, 31*, 1056-1062.

Elias, L., Fenouillot, F., Majeste, J., & Cassagnau, P. (2007). Morphology and rheology of immiscible polymer blends filled with silica nanoparticles. *Polymer, 48*, 6029-6040.

Etika, K. C., Liu, L., Hess, L. A., & Grunlan, J. C. (2009). The influence of synergistic stabilization of carbon black and clay on the electrical and mechanical properties of epoxy composites. *Carbon, 47*, 3128-3136.

Franchini, E., Jocelyne, G., & Gérard, J.-F. (2009). Sepiolite-based epoxy nanocomposites: Relation between processing , rheology, and morphology. *Journal of Colloid and Interface Science, 329*, 38-47.

Harper, C. (2006). *Handbook of Plastic Technologies.* McGraw-Hill.

Irfan, M., & Kumar, D. (2008). Recent advances in isotropic conductive adhesives for electronics packaging applications. *International Journal of Adhesion & Adhesives, 28*, 362-371.

Khoee, S., & Hassani, N. (2010). Adhension strength improvement of epoxy resin reinforced with nanoelastomeric copolymer. *Materials Science & Engineering A, 527*, 6562-6567.

Kim, J., Seong, S., Kang, T., & Youn, J. (2006). Effects of surface modification on rheological and mechanical properties of CNT/epoxy composites. *Carbon, 44*, 1898-1905.

Kim, J.-H., & Jeong, H.-Y. (2005). A study on the material properties and fatigue life of natural rubber with different of carbon blacks. *International Journal of Fatigue 27*, 263-272.

Kotsilkova, R., Fragiadakis, D., & Pissis, P. (2005). Reinforcement effect of carbon nanofillers in an epoxy resin system: rheology, molecular dynamics, and mechanical studies. *J polym Sci Part B Polym Phys, 43*, 522-533.

Luo, Y., Li, Z., & Lan, W. (2007). Response behavior of and epoxy resin/amine curing agent/carbonblack composite film to various solvents. *Materials Science and Engineering B, 139*, 105-117.

Lyon, F., & Burgess, K. (1985). *Encyclopedia of Polymer Science and Engineering* (2nd ed., Vol. 2). New York: John Wiley & Sons.

Shahzada, A., Bohidar, H., & Agnihotry, S. (2006). Role of fumed silica on ion conduction and rheology in nanocomposite polymeric electrolytes. *Polymer*, 3583-3590.

Silva, A. A., Dahmouche, K., & Soared, B. G. (2011). Nanostructure and dynamic mechanical properties of silane-fuctionalized montmorillonite/epoxy nanocomposites. *Applied Clay Science, 54*, 151-158.

Song, Y., & Youn, J. (2005). Influence of dispersion states of carbon nanotubes on physical properties of epoxy nanocomposites. *Carbon, 43*, 1378-1385.

Tao, Z., Yang, S., Ge, Z., Chen, J., & Fan, L. (2006). Synthesis and properties of novel fluorinated epoxy resins based on 1,1-bis(4-glycidylesterphenyl)-1-(3'-trifluoromethylphenyl)-2,2,2-trifluoroethane. *European Polymer Journal, 43*, 550-560.

Wen, X., Wang, Y., Gong, J., Liu, J., Tian, N., Wang, Y., et al. (2012). Thermal and flammability properties of polypropylene/carbon black nanocomposites. *Polymer Degradation and Stability, 97*, 793-801.

Wu, D., Wu, L., Zhang, M., & Wu, L. (2007). Effect of epoxy resin on rheology of polycarbonate/clay nanocomposites. *European Polymer Journal, 43*, 1635-1644.

Wyss, H. M., Larsen, R. J., & Weitz, D. A. (2007). Oscillatory Rheology: Measuring the Viscoelastic Behaviour of Soft Materials. *GIT laboratory journal Europe, 11*, 68-70 .

Zhang, W., Blackburn, R. S., & Dehghani-Sanij, A. (2007). Electrical conductivity of epoxy resin-carbon vlack-silica nanocomposites: Effect of silica concentration and analysis of polymer curing reacting by FTIR. *Scripta materialia, 57*, 949-952.

APPENDICES

APPENDIX A: Results of Rheometer

Time (s)	Log Viscosity 0% (Pa.s)	Log Viscosity 1% N550 (Pa.s)	Log Viscosity 2% N550 (Pa.s)	Log Viscosity 3% N550 (Pa.s)	Log Viscosity 4% N550 (Pa.s)	Log Viscosity 5% N550 (Pa.s)
3	-0.07469	-0.10735	0.021189	0.025306	0.20412	0.31597
6	-0.06702	-0.10237	0.021189	0.033424	0.206826	0.507856
9	-0.05355	-0.09963	0.025306	0.08636	0.212188	0.350248
12	-0.04431	-0.09474	0.029384	0.041393	0.217484	0.33646
15	-0.04769	-0.09259	0.029384	0.045323	0.217484	0.338456
18	-0.05012	-0.09151	0.029384	0.049218	0.220108	0.340444
21	-0.05404	-0.08778	0.037426	0.056905	0.222716	0.344392
24	-0.05061	-0.08407	0.037426	0.060698	0.225309	0.356026
27	-0.04287	-0.08092	0.041393	0.064458	0.230449	0.361728
30	-0.03716	-0.07831	0.041393	0.068186	0.235528	0.359835
33	-0.04191	-0.0804	0.045323	0.071882	0.238046	0.359835
36	-0.04576	-0.08092	0.045323	0.071882	0.240549	0.363612
39	-0.04576	-0.07988	0.049218	0.075547	0.243038	0.361728
42	-0.04144	-0.08197	0.049218	0.079181	0.243038	0.369216
45	-0.02687	-0.08197	0.049218	0.079181	0.245513	0.374748
48	-0.01323	-0.08092	0.053078	0.082785	0.247973	0.376577
51	-0.01278	-0.08725	0.053078	0.089905	0.25042	0.372912
54	-0.01592	-0.08619	0.053078	0.093422	0.25042	0.367356
57	-0.01682	-0.08145	0.060698	0.093422	0.252853	0.365488
60	-0.01637	-0.08249	0.068186	0.120574	0.25042	0.371068

Time (s)	Log Viscosity 0% 1 hour (Pa.s)	Log Viscosity 1% N550 1 hour (Pa.s)	Log Viscosity 2% N550 1 hour (Pa.s)	Log Viscosity 3% N550 1 hour (Pa.s)	Log Viscosity 4% N550 1 hour (Pa.s)	Log Viscosity 5% N550 1 hour (Pa.s)
3	1.472756	1.176091	1.309630	1.201397	1.387390	1.551450
6	1.480007	1.178977	1.313867	1.209515	1.397940	1.557507
9	1.488551	1.181844	1.318063	1.222716	1.409933	1.563481
12	1.492760	1.184691	1.318063	1.209515	1.408240	1.569374
15	1.496930	1.187521	1.320146	1.214844	1.436163	1.575188
18	1.503791	1.190332	1.324282	1.232996	1.416641	1.580925
21	1.506505	1.193125	1.324282	1.225309	1.423246	1.586587
24	1.510545	1.195900	1.326336	1.232996	1.440909	1.589950
27	1.515874	1.198657	1.330414	1.235528	1.541579	1.595496
30	1.519828	1.201397	1.332438	1.238046	1.439333	1.599883
33	1.522444	1.201397	1.332438	1.235528	1.457882	1.600973
36	1.527630	1.204120	1.334454	1.238046	1.454845	1.604226
39	1.530200	1.206826	1.336460	1.240549	1.469822	1.609594
42	1.531479	1.206826	1.336460	1.240549	1.457882	1.617000
45	1.535294	1.206826	1.338456	1.307496	1.453318	1.619093
48	1.539076	1.212188	1.340444	1.245513	1.457882	1.615950
51	1.540329	1.212188	1.340444	1.245513	1.469822	1.618048
54	1.544068	1.214844	1.342423	1.250420	1.463893	1.623249
57	1.546543	1.214844	1.344392	1.250420	1.462398	1.625312
60	1.546543	1.217484	1.344392	1.250420	1.468347	1.625312

Time (s)	Log Viscosity 0% (Pa.s)	Log Viscosity 1% N774 (Pa.s)	Log Viscosity 2% N774 (Pa.s)	Log Viscosity 3% N774 (Pa.s)	Log Viscosity 4% N774 (Pa.s)	Log Viscosity 5% N774 (Pa.s)
3	-0.07469	-0.00043	0.060698	0.0086	0.037426	0.149219
6	-0.06702	0.0086	0.056905	0.0086	0.037426	0.190332
9	-0.05355	0.017033	0.053078	0	0.037426	0.158362
12	-0.04431	0.029384	0.033424	0	0.041393	0.167317
15	-0.04769	0.037426	0.029384	0.004321	0.045323	0.608526
18	-0.05012	0.033424	0.037426	0.012837	0.045323	0.890421
21	-0.05404	0.033424	0.037426	0.025306	0.053078	0.612784
24	-0.05061	0.029384	0.029384	0.029384	0.056905	0.170262
27	-0.04287	0.033424	0.017033	0.029384	0.089905	0.170262
30	-0.03716	0.045323	0.017033	0.029384	0.064458	0.170262
33	-0.04191	0.045323	0.017033	0.029384	0.064458	0.176091
36	-0.04576	0.041393	0.033424	0.025306	0.064458	0.178977
39	-0.04576	0.041393	0.025306	0.037426	0.071882	0.181844
42	-0.04144	0.045323	0.025306	0.037426	0.071882	0.184691
45	-0.02687	0.053078	0.017033	0.033424	0.501059	0.190332
48	-0.01323	0.064458	0.017033	0.029384	0.075547	0.184691
51	-0.01278	0.071882	0.017033	0.029384	0.079181	0.181844
54	-0.01592	0.075547	0.017033	0.033424	0.075547	0.184691
57	-0.01682	0.071882	0.025306	0.045323	0.079181	0.190332
60	-0.01637	0.068186	0.033424	0.053078	0.079181	0.212188

Time (s)	Log Viscosity 0% 1 hour (Pa.s)	Log Viscosity 1% N774 hour (Pa.s)	Log Viscosity 2% N774 1 hour (Pa.s)	Log Viscosity 3% N774 1 hour (Pa.s)	Log Viscosity 4% N774 1 hour (Pa.s)	Log Viscosity 5% N774 1 hour (Pa.s)
3	1.472756	1.133539	1.371068	1.775246	1.531479	1.737193
6	1.480007	1.136721	1.376577	1.78533	1.534026	1.74351
9	1.488551	1.139879	1.382017	1.792392	1.537819	1.747412
12	1.49276	1.143015	1.385606	1.798651	1.536558	1.753583
15	1.49693	1.143015	1.38739	1.805501	1.537819	1.758912
18	1.503791	1.146128	1.390935	1.813581	1.542825	1.761176
21	1.506505	1.149219	1.394452	1.947434	1.542825	1.766413
24	1.510545	1.149219	1.396199	1.830589	1.546543	1.770115
27	1.515874	1.155336	1.399674	1.83187	1.550228	1.771587
30	1.519828	1.158362	1.403121	1.835056	1.549003	1.777427
33	1.522444	1.158362	1.404834	1.839478	1.550228	1.780317
36	1.52763	1.158362	1.40654	1.843233	1.552668	1.781037
39	1.5302	1.161368	1.41162	1.846955	1.552668	1.78533
42	1.531479	1.161368	1.41162	1.850646	1.555094	1.788875
45	1.535294	1.164353	1.41162	1.863917	1.557507	1.789581
48	1.539076	1.164353	1.414973	1.856729	1.557507	1.793092
51	1.540329	1.167317	1.416641	1.859138	1.558709	1.79588
54	1.544068	1.167317	1.418301	1.864511	1.562293	1.79588
57	1.546543	1.170262	1.423246	1.866287	1.562293	1.798651
60	1.546543	1.170262	1.423246	1.868644	1.569374	1.802089

Log Shear Strain (%)	Log G' 0% (Pa)	Log G" 0% (Pa)	Log G' 1% N550 (Pa)	Log G" 1% N550 (Pa)	Log G' 2% N550 (Pa)	Log G" 2% N550 (Pa)	Log G' 3% N550 (Pa)	Log G" 3% N550 (Pa)	Log G' 4% N550 (Pa)	Log G" 4% N550 (Pa)	Log G' 5% N550 (Pa)	Log G" 5% N550 (Pa)
-2.0013	0	0.942504	2.376577	0.206826	2.468347	0	2.390935	1.292256	2.690196	1.617	2.269513	1.563481
-1.83268	0.993436	1.060698	1.912222	1.889302	2.045323	1.923244	1.904716	1.808211	2.214844	2.089905	1.682145	1.517196
-1.67162	1.100371	-0.26122	1.751279	0.775246	1.662758	1.423246	1.4843	1.260071	1.877947	1.632457	1.403121	1.33646
-1.49894	-1.17328	0.838849	1.274158	1.555094	1.39794	1.436163	1.245513	1.307496	1.613842	1.618048	0.879669	0.760422
-1.3098	0.436163	-1.44129	0.748188	0.677607	0.818226	0.943495	0.710117	0.773055	0.975432	1.209515	0.619093	0.992554
-1.12668	-0.31426	0.517196	0.760422	1.0086	0.796574	0.980912	0.634477	0.950365	0.995635	1.158362	0	0.222716
-0.92445	-0.67366	-0.03763	0	-0.10513	-0.89279	0.290035	-0.95078	-1.38091	0	0.618048	0.257679	0.696356
-0.73283	-0.41005	0.247973	0.290035	0.69897	0.193125	0.674861	-0.10403	0.641474	0.4133	0.79379	0.041393	0.498311
-0.52433	-0.98716	0.068186	-0.00436	0.10721	-0.18177	-0.08672	-0.21681	0.222716	0.136721	-0.27003	0.214844	0.649335
-0.32514	-0.74232	0.257679	-0.20135	0.509203	-0.34008	0.447158	-0.36754	0.503791	-0.09044	0.570543	0.152288	0.544068
-0.11634	-0.56543	0.190332	-0.13549	0.356026	-0.24949	0.238046	-0.18509	0.369216	-0.07676	0.352183	0.170262	0.592177
0.093422	-0.82102	0.240549	-0.41794	0.454845	-0.56384	0.354108	-0.41454	0.454845	-0.34872	0.511883	0.082785	0.576341
0.303196	-0.68613	0.243038	-0.31876	0.426511	-0.39794	0.31597	-0.2668	0.426511	-0.16877	0.460898	0.004321	0.570543
0.521138	-0.88606	0.240549	-0.60906	0.447158	-0.69465	0.342423	-0.56864	0.445604	-0.46597	0.49276	-0.1343	0.559907
0.731589	-0.90309	0.25042	-0.49485	0.447158	-0.6517	0.338456	-0.51428	0.444045	-0.36151	0.487138	-0.1831	0.555094
0.956168	-1.20971	0.235528	-0.80688	0.440909	-0.9914	0.32838	-0.88606	0.439333	-0.6216	0.482874	-0.39254	0.539076
1.164353	-1.27901	0.243038	-0.81248	0.444045	-0.95468	0.332438	-0.83268	0.439333	-0.60033	0.485721	-0.4437	0.532754
1.392697	-1.71897	0.220108	-1.33068	0.419956	-1.29757	0.311754	-2.49621	0.416641	-0.85387	0.466868	-0.75696	0.503791
1.598791	0	0.225309	-1.64589	0.421604	-1.63827	0.30963	-1.97062	0.418301	-1.03433	0.463893	-0.85387	0.498311
1.827369	-2.07572	0.20412	-1.48149	0.404834	-1.53165	0.292256	-2.41794	0.399674	-1.06248	0.445604	-0.98297	0.472756

Log Shear Strain (%)	Log G' 0% 1 hour (Pa)	Log G" 0% 1 hour (Pa)	Log G' 1% N550 1 hour (Pa)	Log G" 1% N550 1 hour (Pa)	Log G' 2% N550 1 hour (Pa)	Log G" 2% N550 1 hour (Pa)	Log G' 3% N550 1 hour (Pa)	Log G" 3% N550 1 hour (Pa)	Log G' 4% N550 1 hour (Pa)	Log G" 4% N550 1 hour (Pa)	Log G' 5% N550 1 hour (Pa)	Log G" 5% N550 1 hour (Pa)
-2.0013	2.68842	0	1.875061	1.149219	2.718502	0	2.60206	0	2.260071	0	2.923762	0.313867
-1.83268	2.264818	2.222716	1.653213	0.424882	2.290035	2.217484	2.149219	2.09691	1.762679	1.925828	2.448706	2.396199
-1.67162	1.845098	1.029384	1.374748	1.396199	1.864511	1.41162	1.741939	1.278754	1.580925	0	2.079181	1.577492
-1.49894	1.671173	1.883661	0.472756	0.451786	1.681241	1.808211	1.55145	1.672098	1.324282	1.705008	1.855519	2.017033
-1.3098	0	1.220108	0.522444	0.975432	0	0.783189	0	0.503791	0	1.383815	0	1.08636
-1.12668	1.25042	1.69897	-0.17198	1.045323	1.201397	1.570543	1.075547	1.40654	1.049218	1.600973	1.401401	1.783189
-0.92445	0.930949	1.475671	0.631444	1.220108	0.725095	1.198657	0.498311	1.064458	0.878522	1.4843	1.012837	1.482874
-0.73283	1.049218	1.630428	0.498311	1.230449	0.91169	1.459392	0.729165	1.32838	0.971276	1.583199	1.149219	1.691965
-0.52433	1.049218	1.576341	0.633468	1.276462	0.866287	1.350248	0.720159	1.227887	1.004321	1.553883	1.130334	1.613842
-0.32514	1.0086	1.634477	0.61066	1.285557	0.806858	1.434569	0.662758	1.30963	0.96895	1.599883	1.08636	1.68842
-0.11634	1.045323	1.630428	0.661813	1.303196	0.85248	1.418301	0.722634	1.290035	0.998259	1.599883	1.127105	1.679428
0.093422	0.929419	1.658011	0.571709	1.318063	0.716838	1.450249	0.592177	1.322219	0.900913	1.623249	1.012837	1.708421
0.303196	0.960471	1.663701	0.583199	1.326336	0.748188	1.453318	0.633468	1.32838	0.920123	1.631444	1.033424	1.71265
0.521138	0.79588	1.670246	0.41162	1.330414	0.572872	1.460898	0.454845	1.33646	0.753583	1.636488	0.877371	1.718502
0.731589	0.795185	1.677607	0.403121	1.33646	0.574031	1.466868	0.451786	1.342423	0.748188	1.643453	0.860937	1.725095
0.956168	0.546543	1.669317	0.133539	1.326336	0.326336	1.459392	0.20412	1.334454	0.49276	1.634477	0.639486	1.717671
1.164353	0.515874	1.673021	0.079181	1.330414	0.278754	1.460898	0.149219	1.33646	0.454845	1.63749	0.618048	1.720986
1.392697	0.201397	1.656098	-0.38091	1.311754	-0.05012	1.444045	-0.18776	1.318063	0.117271	1.619093	0.352183	1.703291
1.598791	0.152288	1.658011	-0.45346	1.311754	-0.10624	1.445604	-0.25026	1.320146	0.064458	1.620136	0.313867	1.705008
1.827369	-0.08145	1.635484	-0.97881	1.290035	-0.383	1.421604	-0.52871	1.296665	-0.1945	1.597695	0.133539	1.681241

Log Shear Strain (%)	Log G' 0% (Pa)	Log G" 0% (Pa)	Log G' 1% N774 (Pa)	Log G" 1% N774 (Pa)	Log G' 2% N774 (Pa)	Log G" 2% N774 (Pa)	Log G' 3% N774 (Pa)	Log G" 3% N774 (Pa)	Log G' 4% N774 (Pa)	Log G" 4% N774 (Pa)	Log G' 5% N774 (Pa)	Log G" 5% N774 (Pa)
-2.0013	0	0.942504	2.79141	1.249198	1.838597	0	2.762978	0	2.414137	0.498586	1.955399	1.089198
-1.83268	0.993436	1.060698	2.340642	2.210586	1.111263	1.354301	2.279895	2.168792	1.972619	1.877199	1.516006	1.381476
-1.67162	1.100371	-0.26122	1.96853	1.742725	1.157759	0.340047	1.907089	1.686815	1.542452	1.313656	1.041393	0.781396
-1.49894	-1.17328	0.838849	1.700011	1.709355	0.084576	0.996731	1.665206	1.676511	1.412293	1.396374	0.846894	0.944088
-1.3098	0.436163	-1.44129	1.145507	1.274158	0	0.42586	1.065953	1.313234	0.72583	0.97109	-0.2488	0.414137
-1.12668	-0.31426	0.517196	1.044148	1.245019	0.233757	0.54295	1.068928	1.201943	0.721646	0.982135	0.446382	0.521138
-0.92445	-0.67366	-0.03763	-0.08307	0.809425	-0.08895	0.108903	-0.32175	0.814581	0	0.019947	-0.70224	0.393224
-0.73283	-0.41005	0.247973	0.41797	0.807941	-0.01511	0.363236	0.415641	0.810098	0.147367	0.683767	0.01494	0.55206
-0.52433	-0.98716	0.068186	0	0.143639	-0.19688	0.042969	0	0.033826	-0.0733	0.172019	-0.02319	0.374565
-0.32514	-0.74232	0.257679	-0.2044	0.493737	-0.54151	0.248464	-0.27679	0.52009	-0.1738	0.524136	-0.07707	0.5027
-0.11634	-0.56543	0.190332	-0.10913	0.009451	-0.52622	0.173478	-0.1349	0.057666	-0.1224	0.384174	-0.08276	0.470557
0.093422	-0.82102	0.240549	-0.64493	0.327359	-0.8315	0.256958	-0.64628	0.33626	-0.31903	0.472025	-0.22827	0.511482
0.303196	-0.68613	0.243038	-0.34669	0.205475	-0.58838	0.2403	-0.33171	0.224792	-0.21453	0.442637	-0.15459	0.505828
0.521138	-0.88606	0.240549	-0.75498	0.262214	-0.84588	0.254548	-0.7665	0.283979	-0.42876	0.458184	-0.32477	0.513617
0.731589	-0.90309	0.25042	-0.5499	0.24403	-0.74232	0.257439	-0.56527	0.266937	-0.37675	0.460748	-0.29999	0.515211
0.956168	-1.20971	0.235528	-0.9594	0.246499	-0.94044	0.246991	-0.88539	0.266937	-0.59946	0.453012	-0.49785	0.507721
1.164353	-1.27901	0.243038	-0.88975	0.247482	-0.97469	0.248954	-0.83923	0.269279	-0.59998	0.454387	-0.49662	0.511081
1.392697	-1.71897	0.220108	-1.59619	0.221153	-1.23657	0.23147	-1.3165	0.242044	-0.91116	0.434409	-0.72909	0.49276
1.598791	0	0.225309	-1.75647	0.223496	-1.35399	0.226342	-1.40983	0.244772	-0.95624	0.435207	-0.80438	0.489537
1.827369	-2.07572	0.20412	-1.4389	0.208173	-1.42957	0.207634	-1.32994	0.227115	-1.08176	0.414137	-0.98758	0.467312

Log Shear Strain (%)	Log G' 0% 1 hour (Pa)	Log G" 0% 1 hour (Pa)	Log G' 1% N774 1 hour (Pa)	Log G" 1% N774 1 hour (Pa)	Log G' 2% N774 1 hour (Pa)	Log G" 2% N774 1 hour (Pa)	Log G' 3% N774 1 hour (Pa)	Log G" 3% N774 1 hour (Pa)	Log G' 4% N774 1 hour (Pa)	Log G" 4% N774 1 hour (Pa)	Log G' 5% N774 1 hour (Pa)	Log G" 5% N774 1 hour (Pa)
-2.0013	2.68842	0	2.45393	1.125156	2.805297	1.061452	2.27738	1.696269	2.040998	0	2.799961	0
-1.83268	2.264818	2.222716	1.997736	1.925261	2.322012	2.267641	1.872855	0	1.605197	1.846585	2.317436	2.357363
-1.67162	1.845098	1.029384	1.593508	1.053463	1.984707	1.579555	1.630021	2.011993	#NUM!	1.467608	1.88666	0
-1.49894	1.671173	1.883661	1.376759	1.548144	1.688865	1.86237	0	1.827499	1.227115	1.6289	1.723538	2.047275
-1.3098	0	1.220108	0	0.629919	1.106531	-0.23943	1.212454	1.947826	0.751664	1.503518	0.547405	1.66764
-1.12668	1.25042	1.69897	0.943445	1.327155	1.178113	1.601408	1.0187	1.905148	1.005181	1.606596	1.364551	1.912116
-0.92445	0.930949	1.475671	0.588608	1.065206	0.653695	1.221153	1.313234	1.952647	0.970161	1.560504	1.217484	1.802089
-0.73283	1.049218	1.630428	0.66764	1.245019	0.903578	1.489818	1.301464	1.958755	0.997386	1.61616	1.277609	1.887392
-0.52433	1.049218	1.576341	0.652246	1.17406	0.878809	1.386321	1.392873	1.978454	1.041393	1.611723	1.317854	1.864808
-0.32514	1.0086	1.634477	0.601843	1.243038	0.830589	1.477266	1.354685	1.998782	0.995898	1.641871	1.264582	1.904824
-0.11634	1.045323	1.630428	0.645619	1.231215	0.877256	1.460898	1.400192	2.01368	1.02735	1.648262	1.306425	1.907841
0.093422	0.929419	1.658011	0.521922	1.257198	0.751895	1.49596	1.300595	2.029384	0.935457	1.666612	1.205475	1.926754
0.303196	0.960471	1.663701	0.557026	1.261976	0.782902	1.501744	1.310693	2.037825	0.957655	1.676236	1.222196	1.933993
0.521138	0.79588	1.670246	0.386321	1.267875	0.589391	1.510679	1.143951	2.042969	0.788168	1.680698	1.061452	1.939519
0.731589	0.795185	1.677607	0.382377	1.274158	0.591955	1.517064	1.1329	2.05038	0.782902	1.687618	1.048053	1.946747
0.956168	0.546543	1.669317	0.135451	1.265525	0.311966	1.509471	0.879555	2.042576	0.515609	1.679064	0.80448	1.93897
1.164353	0.515874	1.673021	0.079181	1.267641	0.262214	1.512818	0.848251	2.046885	0.482159	1.682416	0.776265	1.943445
1.392697	0.201397	1.656098	-0.26696	1.249198	-0.18105	1.495128	0.485437	2.029789	0.127429	1.664924	0.453777	1.926394
1.598791	0.152288	1.658011	-0.3098	1.251151	-0.25563	1.49693	0.434569	2.031004	0.067443	1.665862	0.410102	1.928447
1.827369	-0.08145	1.635484	-0.58303	1.227887	-0.74256	1.474508	0.135451	2.009026	-0.22475	1.643058	0.15137	1.905634

Log Shear Strain (%)	Phase Angle 0% (°)	Phase Angle 1% N550 (°)	Phase Angle 2% N550 (°)	Phase Angle 3% N550 (°)	Phase Angle 4% N550 (°)	Phase Angle 5% N550 (°)
-2.0013	90	0.388	0.00286	4.56	4.83	11.1
-1.83268	49.3	43.5	37.1	38.7	37	34.4
-1.67162	2.49	6.03	29.9	30.8	29.6	40.7
-1.49894	89.4	62.3	47.6	49.1	45.3	37.2
-1.3098	0.761	40.4	53.1	49.2	59.8	67.1
-1.12668	81.6	60.5	56.8	64.2	55.5	90
-0.92445	77	90	86.2	20.4	90	70
-0.73283	77.6	68.7	71.8	79.8	67.4	70.7
-0.52433	85	52.3	51.2	70.1	21.4	69.8
-0.32514	84.3	79	80.7	82.4	77.7	67.9
-0.11634	80	72.1	72	74.4	69.5	69.3
0.093422	85	82.3	83.1	82.3	82.1	72.2
0.303196	83.3	79.8	79	78.5	76.8	74.8
0.521138	85.7	85	84.8	84.5	83.7	78.6
0.731589	86	83.5	84.1	83.7	81.9	79.6
0.956168	87.9	86.8	87.3	87.3	85.5	83.3
1.164353	88.3	86.8	87	87	85.3	84
1.392697	89.3	89	88.6	89.9	87.3	86.9
1.598791	90	89.5	89.4	89.8	88.2	87.4
1.827369	89.7	89.3	89.1	89.9	88.2	88

Log Shear Strain (%)	Phase Angle 0% 1 hour (°)	Phase Angle 1% N550 1 hour (°)	Phase Angle 2% N550 1 hour (°)	Phase Angle 3% N550 1 hour (°)	Phase Angle 4% N550 1 hour (°)	Phase Angle 5% N550 1 hour (°)
-2.0013	0.00286	10.6	0.00286	0.00286	0.00286	0.141
-1.83268	42.3	3.38	40.3	41.5	55.5	41.5
-1.67162	8.71	46.5	19.4	19	0.00286	17.5
-1.49894	58.5	43.6	53.2	52.8	67.4	55.3
-1.3098	90	70.6	90	90	90	90
-1.12668	70.4	86.5	66.8	64.9	74.4	67.5
-0.92445	74.1	75.6	71.4	74.7	76.1	71.3
-0.73283	75.4	79.5	74.2	75.9	76.3	74
-0.52433	73.5	77.2	71.8	72.8	74.3	71.8
-0.32514	76.7	78.1	76.7	77.3	76.8	76
-0.11634	75.4	77.1	74.8	74.9	76	74.3
0.093422	79.4	79.8	79.5	79.4	79.3	78.6
0.303196	78.8	79.8	78.8	78.6	79	78.2
0.521138	82.4	83.1	82.6	82.5	82.5	81.8
0.731589	82.5	83.4	82.7	82.7	82.7	82.2
0.956168	85.7	86.3	85.8	85.8	85.9	85.2
1.164353	86	86.8	86.3	86.3	86.2	85.5
1.392697	88	88.8	88.2	88.2	88.2	87.4
1.598791	88.2	89	88.4	88.5	88.4	87.7
1.827369	88.9	89.7	89.1	89.1	89.1	88.4

Log Shear Strain (%)	Phase Angle 0% (°)	Phase Angle 1% N774 (°)	Phase Angle 2% N774 (°)	Phase Angle 3% N774 (°)	Phase Angle 4% N774 (°)	Phase Angle 5% N774 (°)
-2.0013	90	2.685	0.002865	0.002865	0.696	7.748
-1.83268	49.3	40.24	60.26	37.75	38.76	36.26
-1.67162	2.49	16.08	8.649	31.06	30.57	28.78
-1.49894	89.4	56.02	83.02	45.75	43.95	51.36
-1.3098	0.761	90	90	60.49	60.38	77.74
-1.12668	81.6	67.55	63.87	53.64	61.24	49.91
-0.92445	77	71.54	57.62	85.82	90	85.41
-0.73283	77.6	75.18	67.3	68.04	73.79	73.8
-0.52433	85	73.26	60.09	90	60.39	68.19
-0.32514	84.3	77.13	80.79	80.93	78.66	75.25
-0.11634	80	75.45	78.71	57.31	72.7	74.37
0.093422	85	79.57	85.34	84.06	80.81	79.68
0.303196	83.3	78.84	81.56	74.48	77.58	77.67
0.521138	85.7	82.52	85.47	84.91	82.61	81.75
0.731589	86	82.69	84.29	81.63	81.73	81.3
0.956168	87.9	85.76	86.28	85.97	84.93	84.36
1.164353	88.3	86.29	86.58	85.55	84.96	84.39
1.392697	89.3	88.25	88.05	88.42	87.42	86.57
1.598791	90	88.43	88.49	88.73	87.67	87.09
1.827369	89.7	89.11	88.68	88.41	88.17	87.99

Log Shear Strain (%)	Phase Angle 0% 1 hour (°)	Phase Angle 1% N774 1 hour (°)	Phase Angle 2% N774 1 hour (°)	Phase Angle 3% N774 1 hour (°)	Phase Angle 4% N774 1 hour (°)	Phase Angle 5% N774 1 hour (°)
-2.0013	0.00286	2.685	1.033	14.7	0.002865	0.002865
-1.83268	42.3	40.24	41.42	0.002865	60.16	47.63
-1.67162	8.71	16.08	21.47	67.46	90	0.002865
-1.49894	58.5	56.02	56.15	90	68.37	64.62
-1.3098	90	90	2.582	79.58	79.96	85.66
-1.12668	70.4	67.55	69.33	82.6	75.94	74.18
-0.92445	74.1	71.54	74.85	77.08	75.6	75.41
-0.73283	75.4	75.18	75.47	77.59	76.47	76.2
-0.52433	73.5	73.26	72.74	75.44	74.95	74.15
-0.32514	76.7	77.13	77.29	77.21	77.27	77.11
-0.11634	75.4	75.45	75.38	76.31	76.54	75.94
0.093422	79.4	79.57	79.78	79.42	79.48	79.24
0.303196	78.8	78.84	79.19	79.38	79.18	79.01
0.521138	82.4	82.52	83.16	82.8	82.7	82.46
0.731589	82.5	82.69	83.23	83.11	82.9	82.8
0.956168	85.7	85.76	86.37	86.07	86.07	85.8
1.164353	86	86.29	86.79	86.38	86.39	86.11
1.392697	88	88.25	88.79	88.36	88.34	88.07
1.598791	88.2	88.43	88.99	88.55	88.56	88.26
1.827369	88.9	89.11	89.65	89.23	89.22	88.99

APPENDIX B: Results of XRD

*** Basic Data Process ***

Group : DrTeeTT
Data : 0wt_epoxy

Strongest 3 peaks

no.	peak no.	2Theta (deg)	d (A)	I/I1	FWHM (deg)	Intensity (Counts)	Integrated Int (Counts)
1	3	17.3600	5.10417	100	5.22000	824	191901
2	4	19.9200	4.45362	78	0.00000	640	0
3	5	20.8800	4.25097	62	0.00000	510	0

Peak Data List

peak no.	2Theta (deg)	d (A)	I/I1	FWHM (deg)	Intensity (Counts)	Integrated Int (Counts)
1	12.1000	7.30861	8	1.04000	67	3763
2	13.3600	6.62202	23	1.62000	190	17072
3	17.3600	5.10417	100	5.22000	824	191901
4	19.9200	4.45362	78	0.00000	640	0
5	20.8800	4.25097	62	0.00000	510	0
6	21.9800	4.04065	44	0.00000	365	0
7	23.2800	3.81787	25	0.00000	208	0
8	24.0800	3.69281	17	0.00000	141	0
9	25.0800	3.54779	9	0.00000	74	0
10	25.8200	3.44776	5	0.00000	39	0
11	26.1000	3.41141	4	1.00000	31	1705
12	37.9637	2.36820	20	0.58200	165	4809
13	39.5400	2.27734	4	2.00000	29	2527
14	40.3600	2.23294	5	0.00000	38	0
15	41.6600	2.16622	5	0.00000	42	0
16	42.6200	2.11962	6	2.20000	47	4569
17	44.2170	2.04670	23	0.62060	187	5256
18	45.5270	1.99081	4	1.44600	32	3372
19	64.6623	1.44032	26	0.54730	213	6032
20	77.8263	1.22632	48	0.58440	393	12590

```
          ***  Basic Data Process  ***

# Data Infomation
          Group                : DrTeeTT
          Data                 : 0wt_epoxy
          Sample Nmae          : 0wt_epoxy
          Comment              :
          Date & Time          : 07-23-12 15:34:06

# Measurement Condition
    X-ray tube
          target               : Cu
          voltage              : 40.0 (kV)
          current              : 30.0 (mA)
    Slits
          Auto Slit            : not Used
          divergence slit      :   1.00000 (deg)
          scatter slit         :   1.00000 (deg)
          receiving slit       :   0.30000(mm)
    Scanning
          drive axis           : Theta-2Theta
          scan range           :   10.0000 - 80.0000 (deg)
          scan mode            : Continuous Scan
          scan speed           :    2.0000 (deg/min)
          sampling pitch       :    0.0200 (deg)
          preset time          :    0.60 (sec)

# Data Process Condition
    Smoothing                  [ AUTO ]
          smoothing points     : 51
    B.G.Subtruction            [ AUTO ]
          sampling points      : 51
          repeat times         : 30
    Ka1-a2 Separate            [ MANUAL ]
          Ka1 a2 ratio         : 50 (%)
    Peak Search                [ AUTO ]
          differential points  : 51
          FWHM threhold        : 0.050 (deg)
          intensity threhold   : 30 (par mil)
          FWHM ratio  (n-1)/n  : 2
    System error Correction    [ NO ]
    Precise peak Correction    [ NO ]
```

< Group: DrTeeTT Data: 0wt_epoxy >

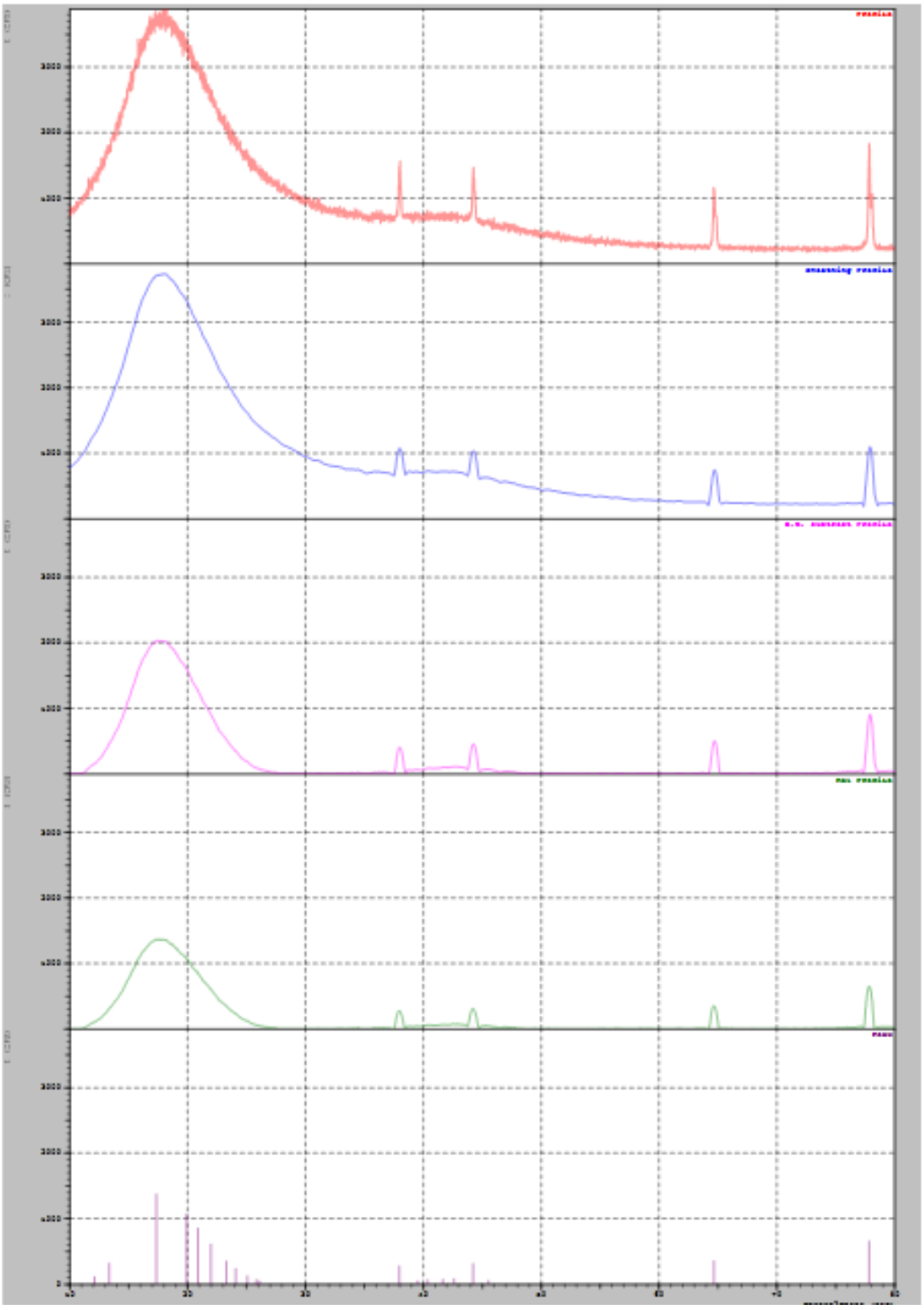

*** Basic Data Process ***

Group : DrTeeTT
Data : 1wt774_epoxy

Strongest 3 peaks

no.	peak no.	2Theta (deg)	d (A)	I/I1	FWHM (deg)	Intensity (Counts)	Integrated Int (Counts)
1	5	17.5800	5.04079	100	0.00000	957	0
2	6	18.4200	4.81277	99	0.00000	948	0
3	7	19.5000	4.54858	87	0.00000	833	0

Peak Data List

peak no.	2Theta (deg)	d (A)	I/I1	FWHM (deg)	Intensity (Counts)	Integrated Int (Counts)
1	11.7600	7.51913	4	0.58000	42	1620
2	13.1200	6.74261	15	1.64000	147	9644
3	14.2400	6.21471	34	2.00000	326	26813
4	15.1400	5.84724	55	0.00000	526	0
5	17.5800	5.04079	100	0.00000	957	0
6	18.4200	4.81277	99	0.00000	948	0
7	19.5000	4.54858	87	0.00000	833	0
8	20.2200	4.38821	77	0.00000	739	0
9	21.4000	4.14883	57	0.00000	550	0
10	22.2600	3.99045	44	0.00000	419	0
11	23.0000	3.86371	32	0.00000	302	0
12	23.5000	3.78262	25	0.00000	239	0
13	24.1800	3.67776	18	0.00000	177	0
14	25.1600	3.53669	10	0.00000	96	0
15	25.9000	3.43729	6	1.33340	60	5798
16	38.0066	2.36562	4	0.61330	43	1542
17	41.3800	2.18023	5	2.96000	48	6445
18	42.3200	2.13395	6	0.00000	53	0
19	43.3200	2.08698	6	0.00000	58	0
20	44.2900	2.04350	10	0.90000	93	6210
21	45.4800	1.99276	5	0.00000	45	0
22	46.6400	1.94586	3	1.54000	31	4436
23	64.6502	1.44056	8	0.54620	79	2162
24	77.8240	1.22635	19	0.58470	181	6068

```
          ***  Basic Data Process  ***

# Data Infomation
          Group                : DrTeeTT
          Data                 : 1wt774_epoxy
          Sample Nmae          : 1wt774_epoxy
          Comment              :
          Date & Time          : 08-01-12 13:16:03

# Measurement Condition
    X-ray tube
          target               : Cu
          voltage              : 40.0 (kV)
          current              : 30.0 (mA)
    Slits
          Auto Slit            : not Used
          divergence slit      :   1.00000 (deg)
          scatter slit         :   1.00000 (deg)
          receiving slit       :   0.30000(mm)
    Scanning
          drive axis           : Theta-2Theta
          scan range           :   10.0000 - 80.0000 (deg)
          scan mode            : Continuous Scan
          scan speed           :    2.0000 (deg/min)
          sampling pitch       :    0.0200 (deg)
          preset time          :    0.60 (sec)

# Data Process Condition
    Smoothing                  [ AUTO ]
          smoothing points     : 51
    B.G.Subtruction            [ AUTO ]
          sampling points      : 51
          repeat times         : 30
    Ka1-a2 Separate            [ MANUAL ]
          Ka1 a2 ratio         : 50 (%)
    Peak Search                [ AUTO ]
          differential points  : 51
          FWHM threhold        : 0.050 (deg)
          intensity threhold   : 30 (par mil)
          FWHM ratio  (n-1)/n  : 2
    System error Correction    [ NO ]
    Precise peak Correction    [ NO ]
```

< Group: DrTeeTT Data: lwt774_epoxy >